NeuroImage xxx (2017) 1–18

Contents lists available at ScienceDirect

NeuroImage

journal homepage: www.elsevier.com/locate/neuroimage

A review on automatic fetal and neonatal brain MRI segmentation

Antonios Makropoulos [a,*], Serena J. Counsell [b], Daniel Rueckert [a]

[a] Biomedical Image Analysis Group, Department of Computing, Imperial College London, London, SW7 2AZ, United Kingdom
[b] Centre for the Developing Brain, Division of Imaging Sciences and Biomedical Engineering, King's College London, London, SE1 7EH, United Kingdom

A B S T R A C T

In recent years, a variety of segmentation methods have been proposed for automatic delineation of the fetal and neonatal brain MRI. These methods aim to define regions of interest of different granularity: brain, tissue types or more localised structures. Different methodologies have been applied for this segmentation task and can be classified into unsupervised, parametric, classification, atlas fusion and deformable models. Brain atlases are commonly utilised as training data in the segmentation process. Challenges relating to the image acquisition, the rapid brain development as well as the limited availability of imaging data however hinder this segmentation task. In this paper, we review methods adopted for the perinatal brain and categorise them according to the target population, structures segmented and methodology. We outline different methods proposed in the literature and discuss their major contributions. Different approaches for the evaluation of the segmentation accuracy and benchmarks used for the segmentation quality are presented. We conclude this review with a discussion on shortcomings in the perinatal domain and possible future directions.

1. Introduction

Automated morphometric analysis of the perinatal brain is essential to quantitatively assess normal brain development and investigate the neuroanatomical correlates of cognitive impairments. Several neurological deficits have been associated with abnormalities in the developing brain, presenting a window for therapeutic intervention. Approximately 10% of infants who are born preterm will develop cerebral palsy (Hack and Fanaroff, 2000) and up to 50% will develop cognitive and/or behavioural problems in childhood (Marlow et al., 2005; Delobel-Ayoub et al., 2009). Problematic cases can be traced back as early as the fetal age. Ventriculomegaly, the enlargement of the cerebral ventricles, is the most common abnormality in the fetal brain and has been associated with neurological conditions such as schizophrenia, autism and epilepsy (Wright et al., 2000; Palmen et al., 2005; Jackson et al., 2011).

With advances in Magnetic Resonance Imaging (MRI), detailed images of the fetal and neonatal brain can be visualized non-invasively at a millimeter scale. Quantitative neuroimaging studies using MRI are increasingly being used to assess brain growth and development in the perinatal period. The segmentation of the brain in MRI is a prerequisite to derive quantitative measurements of regional brain structures. Regional volumetric and shape measurements of the brain are derived on the basis of the segmented structures of the brain. Segmentations overlaid on images are further important for visualization purposes. Diffusion weighted imaging (DWI) and functional MRI (fMRI) can be used together with segmentations from structural MRI to compute regional measurements relating to structural and functional brain connectivity. Systematic assessment of these measurements in population studies is essential to identify regions of the brain that are affected by pathologies and provide information on the normal development of the brain.

Quantitative measurements of volume and cortical surface are important to characterise normal brain development and have the potential to predict long-term neurodevelopmental performance (Peterson et al., 2003; Counsell et al., 2008; Thompson et al., 2008; Rathbone et al., 2011; Boardman et al., 2010). However, manual segmentation of MR images is extremely time consuming and thus an expensive process. Furthermore, manual labelling is subject to inter- and intra-observer variability, which limits its reproducibility. These limitations of manual approaches present an obstacle in labelling large cohorts of subjects that are required for population studies. There is therefore a need for accurate automatic techniques to parcellate the brain into structures of interest. Automatic segmentation of the neonatal and fetal brain is considerably more challenging than the adult brain. MR images of the perinatal brain have a much lower contrast-to-noise ratio (CNR), frequently have lower signal-to-noise ratio due to the small size of the brain and vary enormously in terms of brain shape and appearance as a result of rapid brain development during this period. They are further subject to significant motion artifacts of the infants during the image acquisition.

The aim of this study is to provide a comprehensive review of techniques used for the automatic segmentation of the fetal and neonatal

* Corresponding author.
E-mail address: a.makropoulos11@imperial.ac.uk (A. Makropoulos).

http://dx.doi.org/10.1016/j.neuroimage.2017.06.074
Received 1 November 2016; Received in revised form 6 March 2017; Accepted 26 June 2017
Available online xxxx

brain. A recent review by Devi et al. (2015) presented segmentation techniques developed for the neonatal brain. Here we provide an extended review for both the fetal and neonatal period. Additionally, we provide a summary of existing atlases for this period, a detailed classification of techniques based on the methodology and an extensive list of future directions. An initial list of methods included in this review was compiled using PubMed.[1] Relevant methods were detected searching for the terms "fetal brain MRI segmentation" and "neonatal brain MRI segmentation". Methods that participated in NeoBrainS12, a recent challenge that is presented in Section 9.1, were further included in the review. Finally, relevant methods referenced from the included studies were further considered for inclusion. This paper reviews automatic techniques, therefore methods that require human interaction were excluded. The methods were categorised according to the target population (fetal, neonatal), structures segmented (brain, tissues, regional structures) and the methodology adopted (unsupervised, parametric, classification, atlas fusion, deformable models).

The paper is organised as follows. The challenges in automatic segmentation of the developing brain are discussed in Section 2. Atlases that are typically provided as prior information for the segmentation are presented in Section 3. Sections 4 and 5 briefly outline image acquisition and preprocessing techniques used prior to the segmentation. Section 6 introduces the categories that the different methods are classified into in this review. Sections 7 and 8 present the different segmentation methods proposed in the fetal and neonatal literature. Evaluation of the segmentation techniques is presented in 9. Finally, we conclude and discuss possible future directions in the field.

2. Challenges

Despite advances in the acquisition of MR images, automatic brain segmentation is still demanding. There are significant challenges in the MR images that hinder the segmentation irrespective of the application at hand. The intensity of the different tissue classes is not uniform, rather changes gradually, over the image space. This intensity inhomogeneity/non-uniformity (INU) is caused by non-uniform radio-frequency (RF) fields and reception sensitivity as well as electromagnetic interaction with the body (Belaroussi et al., 2006). Higher field strength scanners result in more significant intensity variability. Fig. 1 demonstrates the INU effect. Partial Volume (PV) effects, the mixing of different tissue classes in a single voxel (Tofts, 2003), pose additional difficulties for the accurate delineation of the tissue boundaries. Since the image resolution is limited, voxels that contain more than one tissue result in an intensity that represents the mixture of tissues in the voxel. Noise in the image is further often evident and can be due to electromagnetic noise in the body and small anomalies in the reception electronics (Weishaupt et al., 2008).

Automatic segmentation of fetal and neonatal brain MRI is considerably more challenging than adult brain segmentation. The perinatal brain MR images further exhibit domain-specific challenges:

a) Increased occurrence of motion artifacts compared to the adults. The fetuses and unsedated neonates demonstrate significant motion, that necessitate adoption of faster acquisitions or multiple acquisitions of the brain to correct for the motion. Motion artifacts appear as misaligned image slices and ghosting effects along the direction of phase-encoding (Rutherford, 2002) (an example is presented in Fig. 2).
b) Lower contrast-to-noise ratio (CNR) due to the small size of the fetal/neonatal brain and shorter scanning periods (Prastawa et al., 2005).
c) CSF-WM PV. The fetal/neonatal MR images exhibit an inverted WM/GM contrast compared to the adult data. The WM, which is predominantly unmyelinated in the perinatal brain, appears brighter than GM in the T2-weighted images while in the adult data GM has larger intensity values than WM. The mixing of CSF and GM in the CSF-CGM boundary leads to intensities similar to the intensity profile of the WM (see Fig. 3). This PV effect leads to mislabelled PV voxels as WM in the CSF-CGM interface (Xue et al., 2007).
d) Perinatal brains vary enormously in shape and appearance of structures due to the rapid brain development during this period. The cortical ribbon is rapidly folding and deep GM structures are formed. Furthermore, WM myelination is an ongoing process in the developing brain and is progressively evident at different WM regions. The precise registration of subjects of different scan ages is challenging due to these differences in anatomical characteristics. Fig. 4 exhibits the changes occurring with increasing scan age in the neonatal brain.
e) Lack of manually-labelled atlases across different scan ages. Manual delineation of detailed structures requires expert anatomical knowledge and is extremely time-consuming. Contrary to the atlas resources that exist for the adult brain, manual brain atlasing during the perinatal period is very limited. The large variability in brain appearance in addition to the lack of atlases poses a challenge to segmentation techniques as the training data are scarce.

3. Atlases

Atlases are labelled data that specify the location of different structures of the brain and are commonly used as paradigm for automatic segmentation algorithms. The term atlas is often used in an ambiguous fashion. In the context of this review we will use the term atlas to refer to a pair of images: one being the atlas template image (e.g. an MR image of the brain) and one being the atlas label image. The atlas label image indicates the presence of anatomical structures or tissues at every voxel. There are two types of atlases: single-subject atlases that assign a single structure/tissue label at each voxel and probabilistic atlases that define the structure probability of each structure/tissue at each voxel. Single-subject atlases are usually manually delineated while probabilistic atlases are typically formed by averaging automatically-derived segmentations.

The labels of an atlas can be propagated to an unlabelled subject by registering the MR image of the atlas (source) to the MR image of the subject (target). The registration estimates a transformation, a mapping, between the images that maximises the similarity between the source and the target image. The registration can be global or local and estimates a linear (rigid or affine motion) or non-linear transformation (local motion) respectively, of the source to the target image. The estimated transformation can then be used to transform/warp the atlas image and labels to the subject space.

Early atlas-based segmentation approaches segmented the target image by propagating the labels of a single manually labelled atlas (Christensen et al., 1994; Collins et al., 1995). However, by using a single atlas, the segmentation is limited to the accurate registration of a single pair of brains, which is a non-trivial problem due to the large differences in the anatomy of the subjects. Probabilistic atlases were introduced to address this limitation. Probabilistic atlases are constructed by averaging the intensity images and corresponding segmentations over a large number of subjects. Registration of a subject to an average template is typically less challenging than registration to a subject MRI since large differences in anatomy have been smoothed out as a result of the averaging. Additionally, probabilistic atlases provide a probabilistic estimate of each structure at every voxel. This is essential for probabilistic segmentation approaches that require a prior probability model for each label e.g. Van Leemput et al. (1999). Another alternative to address the inaccuracy from the registration of a single atlas is the use of multiple atlases, where different atlases are independently registered to the subject. This allows for errors introduced by a single atlas to be averaged out using the majority of the atlases, and improves the accuracy of the result (Rohlfing et al., 2004; Heckemann et al., 2006). Typically either multiple single-subject atlases or probabilistic atlases are used for segmentation to accommodate the anatomical variability exhibited in the brain.

[1] https://www.ncbi.nlm.nih.gov/pubmed.

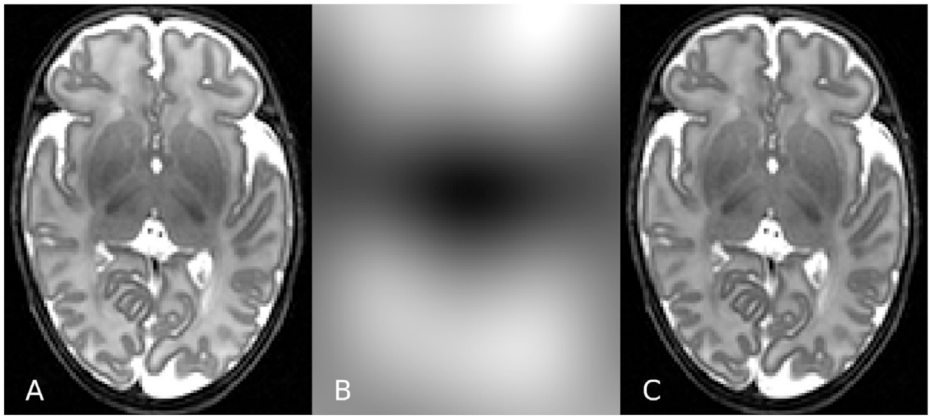

Fig. 1. MRI intensity inhomogeneity exhibited on a neonatal T2 MR image (A). Images (B) and (C) present the estimated bias field and bias-corrected image, respectively, using the N4 bias field correction (Tustison et al., 2010).

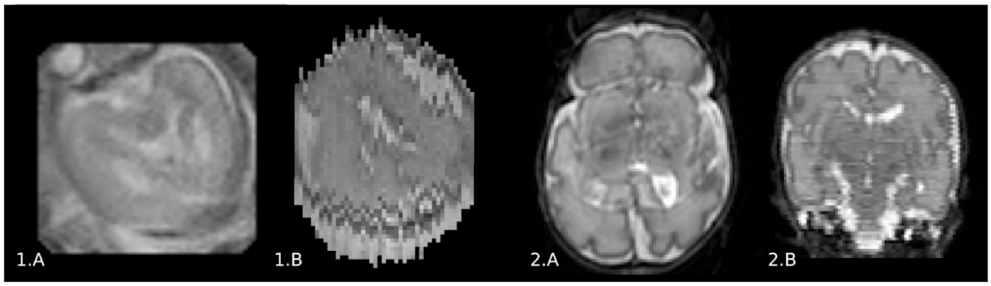

Fig. 2. Motion artifacts on a fetal (1) and a neonatal (2) T2 MR image. Motion is evident with blurring and ghosting effects in the slices of the phase encoding direction (1.A, 2.A) and misalignment of the slices along the direction (1.B, 2.B).

The following sections present single-subject and probabilistic atlases existing in the neonatal and fetal domain. Table 1 summarises the different atlases. Table 3 further presents publicly available atlases for the perinatal brain.

3.1. Single-subject atlases

There are limited single-subject atlases constructed in the literature for the perinatal brain. Oishi et al. (2011),[1] constructed a multi-channel neonatal atlas consisting of T1, T2 and DTI intensities and a manual delineation of 122 regions on a single subject. The delineation was based on the white matter tracts and gyral patterns observed on the DTI data. Gousias et al. (2012),[2] in contrast produced multiple single-subject atlases based on T1 and T2 data. They manually delineated 50 structures on 20 neonates at different scan ages around term age (an example atlas of Gousias et al. (2012) is illustrated in Fig. 5). de Macedo Rodrigues et al. (2015) constructed multiple single-subject atlases at different ages using T1 scans. Brain MR images of 23 infants with scan age between 0 and 2 years of age, including 4 neonates, were manually parcellated into 32 regions. A recent atlas was constructed by Alexander et al. (2016) that delineates 100 regions in the T2 scans of 10 term-born neonates. An important characteristic of this atlas is that it replicates the Desikan-Killiany protocol (Desikan et al., 2006), that is widely used in adult studies, for the neonatal brain (see Fig. 6).

3.2. Probabilistic atlases

Several probabilistic atlases have been constructed for the neonatal brain. Kuklisova-Murgasova et al. (2011) used non-parametric kernel regression to construct the first spatio-temporal atlas of the neonatal brain between the ages at scan of 28–44 weeks. They computed average T1 and T2 templates based on 142 images that were affinely registered to a common space. Each age of the template is further accompanied by tissue probability maps estimated from automatic tissue segmentations of the subjects. Serag et al. (2012) used a similar approach to develop a "high-definition" atlas with spatio-temporal templates and tissue probability maps. Their atlas was based on non-linear pairwise registration (pairwise free-form deformations) of 204 subjects, instead of one-way affine registrations used in Kuklisova-Murgasova et al. (2011). Schuh et al. (2015) followed the same principles however used a different registration method (symmetric registration between source and target that produces inverse-consistent transformations) to create an atlas from 28 to 44 weeks using 118 neonatal scans. Makropoulos et al. (2016)

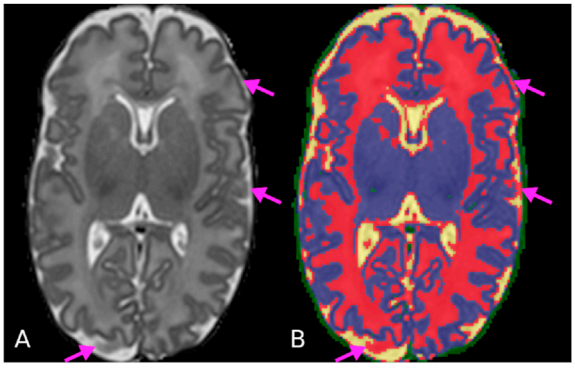

Fig. 3. CSF-WM PV evident in the CSF-CGM boundary. A neonatal T2 MR image (A) is split into tissues types (yellow:CSF, red:WM, blue:GM, green:background) with intensity clustering (B). The arrows point areas where the partial volume of CSF and CGM results in similar intensities to the WM.

[2] http://www.developingconnectome.org/.

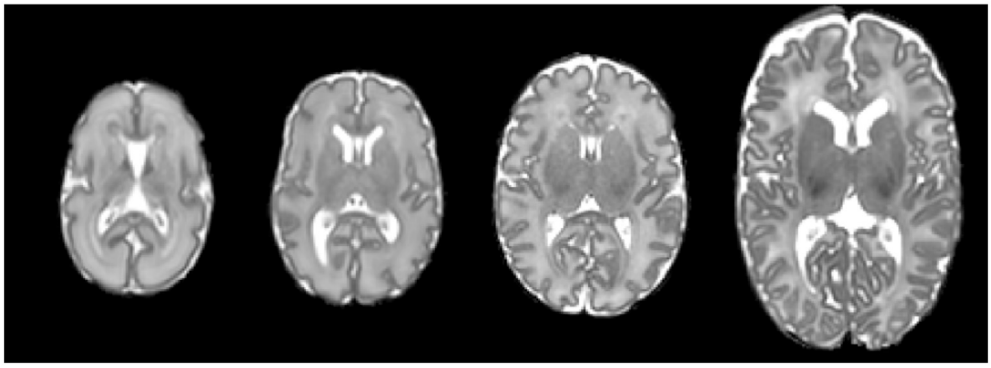

Fig. 4. T2 MR images of the neonatal brain acquired at 28,32,36 and 44 weeks PMA (from left to right).

Table 1
Studies related to atlas construction for the fetal and neonatal brain.

	Templates	Structures	Time-points Subjects	
Single-subject atlases				
Neonatal				
Oishi et al. (2011)[1]	T1,T2,FA,MD	122 regions	1 term	1
Gousias et al. (2012)[2]	T1,T2	50 regions	20 term	20
de Macedo Rodrigues et al. (2015)	T1	32 regions	23 at 0,1,2 years	23
Alexander et al. (2016)	T2	100 regions	10 term	10
Probabilistic atlases				
Fetal				
Habas et al. (2010a)	T2	4 tissues	21-24 weeks GA	20
Serag et al. (2012)	T1,T2	4 tissues	23-37 weeks GA	80
Neonatal				
Kuklisova-Murgasova et al. (2011)	T2	6 tissues	28-44 weeks PMA	142
Shi et al. (2011b)	T1,T2	3 tissues, 90 regions	0,1,2 years	95
Serag et al. (2012)	T1,T2	6 tissues	28-44 weeks PMA	204
Shi et al. (2014)	T2	3 tissues	1 term	73
Schuh et al. (2015)	T2	6 tissues	28-44 weeks PMA	118
Makropoulos et al. (2016)	T1,T2	6 tissues, 87 regions	28-44 weeks PMA	420
Zhang et al. (2016)	T2	3 tissues	1 term	73
Blesa et al. (2016)	T1, T2, FA, MD	3 tissues, 107 regions	1 term	33

enhanced the atlas of Serag et al. (2012) with spatio-temporal probability maps and label maps for 87 structures, estimated from 420 automatically segmented neonatal MR images. Shi et al. (2011b) proposed the first longitudinal atlas with three time-points of the infant brain: neonatal, 1 year and 2 years, based on 95 subjects scanned at the three ages. Longitudinal tissue segmentation, labelling based on the Automated Anatomical Labeling (AAL) atlas (Tzourio-Mazoyer et al., 2002) and groupwise registration were used to compute the three templates (T2 for the neonatal and T1 for the 1-year and 2-years old), tissue probability maps and label maps for 90 structures. More recently, Shi et al. (2014) used a sparse patch-based technique to build an atlas consisting of a T2 template and tissue probability maps. They used MR images of 73 neonates that were aligned with groupwise registration and automatically segmented into the different tissue types with the method proposed in Wang et al. (2011). Zhang et al. (2016) similarly adopted a patch-based methodology after splitting the brain images with wavelet decomposition into different frequency subbands. A T2 template and tissue probability maps are derived using the same number of subjects as Shi et al. (2014). Blesa et al. (2016) produced a multi-modal atlas with a single timepoint with T1, T2, FA, MD templates utilising MR images of 33 subjects. Tissue probability maps were based on automatic segmentations and a label map with 107 labels was constructed based on propagation of labels from the AAL atlas (Tzourio-Mazoyer et al., 2002).

Habas et al. (2010a) constructed the first spatio-temporal atlas of the fetal brain. They used groupwise registration between the subjects and modelled the changes in MR intensity, tissue probability and shape of the fetal brain with polynomials. The atlas utilised T2 images and manual segmentations of 20 fetal brains and was defined at the range of 20–24 weeks gestational age (GA). Serag et al. (2012), in addition to their neonatal atlas, derived a spatio-temporal atlas of the fetal brain and tissue probability maps between 23 and 37 weeks GA based on 80 fetuses.

4. Image acquisition

MR imaging of the perinatal brain requires different acquisition protocols than the protocols used for the adult brain. The immature perinatal brain has higher water content than the adult brain that necessitates different scanning parameters (Counsell and Rutherford, 2002). Additionally, due to patient motion faster scanning sequences, such as fast spin echo techniques, are required to obtain images with reduced motion artifacts. Motion is particularly evident in the fetal brain MRI as a result of both the fetal movement and the maternal breathing.

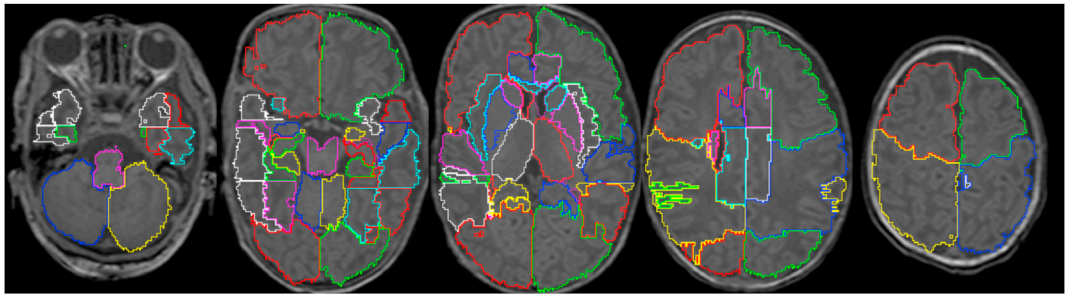

Fig. 5. Atlas manually delineated by Gousias et al. (2012) dividing the brain into 50 regions.

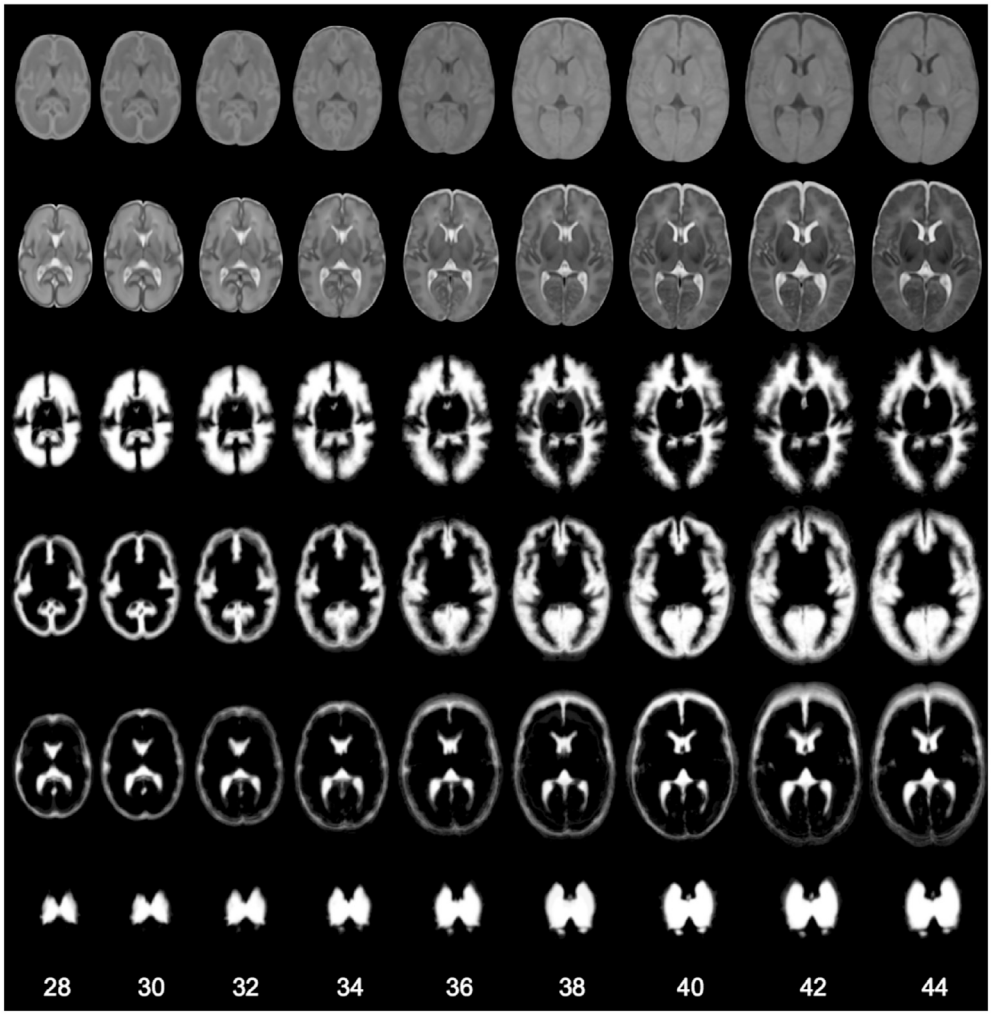

Fig. 6. The spatio-temporal probabilistic atlas of the neonatal brain constructed by Serag et al. (2012).

Fetal brain MRI is often acquired with very fast acquisition of 2D slices that 'freeze' the motion within a slice. However, the 2D slices are often misaligned with each other, hence hampering the automatic brain segmentation. 3D reconstruction techniques are often used to correct for such misalignments (Rousseau et al., 2006; Jiang et al., 2007; Gholipour et al., 2010; Kim et al., 2010; Kuklisova-Murgasova et al., 2012; Cordero-Grande et al., 2016). Slice-to-volume (SVR) techniques (Rousseau et al., 2006; Jiang et al., 2007; Gholipour et al., 2010; Kuklisova-Murgasova et al., 2012; Cordero-Grande et al., 2016) usually perform this correction in two iterative steps: a) 3D reconstruction from the 2D slices and b) re-alignment of the 2D slices to the 3D volume. Alternative reconstruction techniques align the slices by optimizing the intersections of all slice pairs (Kim et al., 2010). Numerous motion correction techniques have been proposed in the literature to correct for the inherent motion either prospectively during the acquisition, or retrospectively as part of the reconstruction from the k-space. A comprehensive survey of the different motion correction techniques is presented in Zaitsev et al. (2015).

5. Image preprocessing

Different preprocessing steps are often adopted prior to the segmentation. The most common are intensity correction and brain extraction. Intensity inhomogeneity (INU) correction aims to remove the intensity bias exhibited as a smooth varying signal across the image. INU correction can be performed prior to the segmentation and/or inherently in the segmentation process. The N3 (Sled et al., 1998) and N4 algorithms (Tustison et al., 2010) are commonly used to perform INU correction in the perinatal brain (Makropoulos et al., 2014; Wu et al., 2014; Tourbier et al., 2015; Wang et al., 2015; Rajchl et al., 2016; Serag et al., 2016). Filtering techniques such as anisotropic diffusion have been further employed in the literature to reduce noise in the images while preserving the edges (Prastawa et al., 2005; Weisenfeld and Warfield, 2009; Gui et al., 2012b). Tissue and structural segmentation methods often initially perform brain extraction prior to processing. In this review, we outline brain extraction techniques as a special category of segmentation methods and describe them in Sections 7.1 and 8.1 for the fetal and neonatal brain.

6. Segmentation categories

The segmentation techniques in this review are categorised according to:

a) the target population into fetal or neonatal.
b) the structures segmented into brain, tissue or structural segmentation methods.
c) and the methodology adopted into unsupervised, parametric, classification, atlas fusion, deformable models.

The methodology categories are detailed in the following sections. Sections 7 and 8 consequently present in detail the techniques proposed in the fetal and neonatal literature respectively for the different

categories. Table 2 displays the different segmentation methods discussed in this review with respect to their category. Table 3 presents publicly available methods discussed in this review.

6.1. Unsupervised techniques

The unsupervised techniques classify the data according to some measure of inherent similarity and do not require training data. Unsupervised techniques in the segmentation domain incorporate methods that exploit image-derived features to split the image into intensity-distinct regions. Methods used in medical image segmentation are sometimes adopted from standard image processing: thresholding (Al-Attas and El-Zaart, 2007), region growing (Adams and Bischof, 1994; Justice and Stokely, 1996), morphological operations (Mangin et al., 1995), watershed segmentation (Sijbers et al., 1997), edge detection (Yuqian et al., 2005) and clustering techniques (Macqueen, 1967; Bezdek, 1981). Further details on the aforementioned techniques can be found in textbooks on image processing, e.g. Pitas (2000); Pratt (2007); Bankman (2008). Unsupervised techniques on their own are highly susceptible to noise, intensity inhomogeneity and partial volume averaging and therefore hard to adapt to different scanning sequencies and large anatomical differences. In the perinatal segmentation literature, these methods have been mainly used for pre-processing and post-processing purposes of other methods e.g. parametric techniques. Clustering techniques have been employed to compute subject-specific tissue priors to initialise parametric techniques (Xue et al., 2007; Shi et al., 2010; Makropoulos et al., 2012a; Melbourne et al., 2012). Region growing, morphological operations and watershed segmentation have been used to identify/separate connected regions in the image (Anquez et al., 2009; Péporté et al., 2011; Gui et al., 2012b; Keraudren et al., 2014) and correct for partial volume voxels from overlapping tissue intensity distributions e.g. between WM and CSF or CGM and background (Xue et al., 2007; Makropoulos et al., 2012a; Wang et al., 2012c; Wu and Avants, 2012; Beare et al., 2016). However, combination of unsupervised techniques have been also successfully adopted for brain and tissue segmentation (Péporté et al., 2011; Gui et al., 2012b).

6.2. Atlas fusion techniques

Atlas fusion approaches are methods that segment the image based on the labels of aligned atlases. Label fusion techniques combine the label votes from different atlases (Rohlfing et al., 2004; Heckemann et al., 2006). Different voting schemes have been proposed that weight the contribution of each atlas according to the similarity of the atlas MR image to the unseen image, either globally or locally (Artaechevarria et al., 2009). Patch-based techniques (Coupé et al., 2011; Rousseau et al., 2011) provide a non-local alternative to the label fusion techniques. In patch-based methods the most similar patches in the atlases are located for each voxel of the image, at the neighborhood of the voxel. The labels of the patches are fused with a weight defined by the similarity of the atlas patch to the image patch around the voxel. The weighting can be further refined in order to reduce the joint atlas errors between different atlases as shown in Wang et al. (2012a). Another family of atlas fusion techniques, STAPLE (Simultaneous Truth and Performance Level Estimation), was proposed by Warfield et al. (2004). STAPLE computes an estimate of the true segmentation and weights the atlases according to their performance to the estimated segmentation. The procedure is repeated until convergence in an EM framework. In the perinatal

Table 2
Segmentation methods discussed in this review by category.

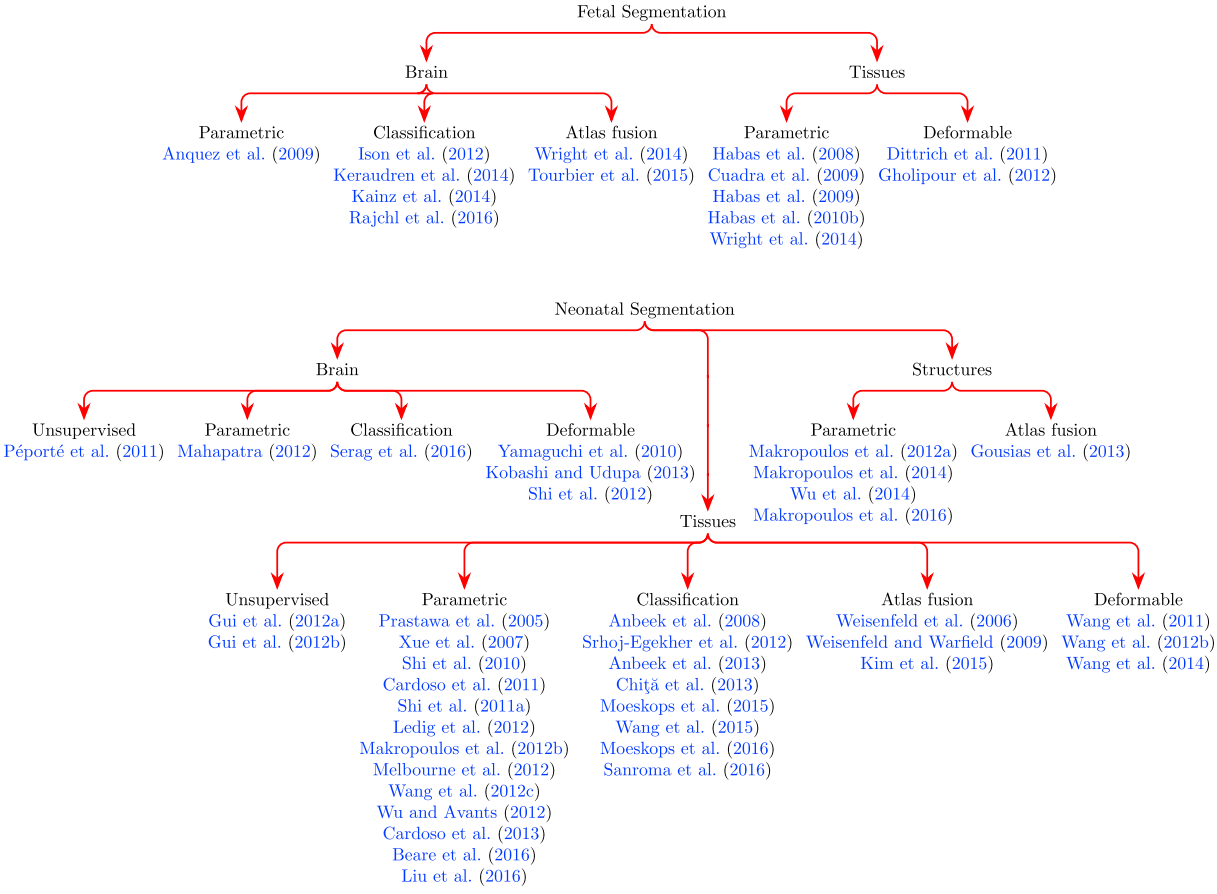

Table 3
Publicly available atlases and software for brain MRI segmentation.

Atlases	
Habas et al. (2010a)	http://depts.washington.edu/bicg/research/fba.php
Oishi et al. (2011)	http://cmrm.med.jhmi.edu/cmrm/Data_neonate_atlas/atlas_neonate.htm
Shi et al. (2011b)	https://www.med.unc.edu/bric/ideagroup/free-softwares/unc-infant-0-1-2-atlases
Kuklisova-Murgasova et al. (2011)	http://brain-development.org/brain-atlases/neonatal-brain-atlas
Serag et al. (2012)	http://brain-development.org/brain-atlases/consistent-high-definition-spatio-temporal-neonatal-brain-atlas
Serag et al. (2012)	http://brain-development.org/brain-atlases/a-multi-channel-4d-probabilistic-atlas-of-the-developing-fetal-brain
Gousias et al. (2012)	http://brain-development.org/brain-atlases/neonatal-brain-atlas-albert
Makropoulos et al. (2016)	http://brain-development.org/brain-atlases/multi-structural-neonatal-brain-atlas
Segmentation software	
Shattuck et al. (2001)	http://brainsuite.org
Smith (2002)	http://fsl.fmrib.ox.ac.uk
Warfield et al. (2004)	https://www.nitrc.org/projects/staple
Ashburner and Friston (2005)	http://www.fil.ion.ucl.ac.uk/spm
Prastawa et al. (2005)	https://www.nitrc.org/projects/neoseg
Avants et al. (2011)	https://github.com/stnava/ANTs
Wang et al. (2011)	http://www.nitrc.org/projects/ibeat
Eskildsen et al. (2012)	https://github.com/fristed/BEaST
Shi et al. (2012)	https://www.nitrc.org/projects/skulltoolkit
Wang et al. (2012a)	https://www.nitrc.org/projects/picsl_malf
Cardoso et al. (2013)	https://sourceforge.net/projects/niftyseg
Keraudren et al. (2014)	https://github.com/kevin-keraudren/example-motion-correction
Makropoulos et al. (2014)	https://github.com/MIRTK/DrawEM
Beare et al. (2016)	https://github.com/DevelopmentalImagingMCRI/mantis

literature, segmentation using solely atlas fusion techniques is relatively limited. This is due to the large developmental changes occurring at different ages at scan and the limited amount of labelled atlases for different ages. Registration between atlases at different age from the subject, e.g. registration of term atlases to early-preterm subjects, is challenging. However, atlas fusion is commonly used to derive initial probability estimates of the different structures, that are consequently refined by adaptive techniques such as parametric or deformable techniques. Patch-based segmentation in the literature has been used in Wright et al. (2014), label fusion in Tourbier et al. (2015); Srhoj-Egekher et al. (2012); Gousias et al. (2013); Sanroma et al. (2016) and STAPLE in Gholipour et al. (2012); Weisenfeld and Warfield (2009); Kim et al. (2015).

6.3. Parametric techniques

Parametric models solve the segmentation problem by fitting a model to the data. The (posterior) voxel probabilities are derived as a composition of a spatial prior term and an intensity term. The spatial prior distribution essentially encodes the spatial location of each structure and is usually derived based on atlases. A typical choice of parametric distribution for the intensity model is the Gaussian mixture model (GMM), where the intensity likelihood of each brain structure is modelled with a Gaussian distribution. The model is then normally fitted to the data with the use of Expectation-Maximization (EM) (Wells et al., 1996; Van Leemput et al., 1999), Iterated Conditional Modes (ICM) (Fischl et al., 2002; Ashburner and Friston, 2005) or graph cuts (Song et al., 2006; van der Lijn et al., 2008). Common extensions of parametric models encompass: MRF regularization to model the spatial interaction of structures (Van Leemput et al., 1999; Fischl et al., 2002), bias field correction to account for the intensity inhomogeneity (Van Leemput et al., 1999; Ashburner and Friston, 2005), and prior relaxation to accommodate mis-registrations and pathologies (Shiee et al., 2011). This family of models has been adopted in the majority of neonatal and fetal segmentation methods due to its accuracy and robustness to differences in anatomy. The intensity modelling allows adaptation of the spatial prior information, typically derived from probabilistic atlases or atlas fusion, according to intensity information of the image. Graph cuts have been used for brain segmentation (Anquez et al., 2009; Mahapatra, 2012) and EM for brain, tissue and structure segmentation (Prastawa et al., 2005; Xue et al., 2007; Habas et al., 2008; Cuadra et al., 2009; Shi et al., 2010; Cardoso et al., 2011; Ledig et al., 2012; Makropoulos et al., 2012b; Wang et al., 2012c; Wu and Avants, 2012; Beare et al., 2016; Liu et al., 2016). EM is often implemented with MRF regularization (Habas et al., 2008; Cuadra et al., 2009; Xue et al., 2007; Cardoso et al., 2011; Ledig et al., 2012; Makropoulos et al., 2012a; Wu and Avants, 2012), bias field correction (Habas et al., 2008; Shi et al., 2010; Cardoso et al., 2011; Ledig et al., 2012; Makropoulos et al., 2012a) and prior relaxation (Cardoso et al., 2011; Makropoulos et al., 2012a).

6.4. Classification techniques

A classifier is directly trained on the atlases to learn the label assignment based on image-derived features, such as the intensity of single or multiple modalities and spatial features. Estimated labels from other segmentation techniques can be further incorporated as features to learn and correct for the segmentation bias of the techniques (Wang et al., 2010). Afterwards, the classifier labels the voxels in the subject image on the basis of the learned model. Classification techniques, especially convolutional neural networks, are amongst the most popular methods for segmentation in recent years due to their outstanding accuracy in computer vision tasks e.g. (Krizhevsky et al., 2012) and trivial adaptation of models across different domains. Example classification techniques in the perinatal literature have employed *k*-NN (Anbeek et al., 2008; Srhoj-Egekher et al., 2012; Chiţă et al., 2013; Moeskops et al., 2015), naive Bayes (Srhoj-Egekher et al., 2012; Serag et al., 2016), decision forests (Ison et al., 2012; Keraudren et al., 2014; Kainz et al., 2014; Wang et al., 2015), SVM classifiers (Moeskops et al., 2015; Sanroma et al., 2016) and more recently convolutional neural networks (CNN) (Moeskops et al., 2016; Rajchl et al., 2016).

6.5. Deformable models

Deformable models are physics-based models that segment an object by deforming a closed surface. The surface is iteratively expanded or contracted under the influence of an external and an internal energy. The external energy is usually an image-driven data fitting term that moves the surface to the desired object boundary. The internal energy ensures the smoothness of the propagating surface and constrains the evolution driven by the external energy. The internal energy may further incorporate prior knowledge about the object of interest. Deformable models are classified into two categories: the parametric and geometric models. Parametric models (Kass et al., 1988; Terzopoulos and Fleischer, 1988) provide an explicit parameterization of the surface. An example method using parametric deformable models is the widely used algorithm for brain extraction, BET, proposed by Smith (2002) (implemented as part of the FSL software). Geometric models (Osher and Sethian, 1988; Malladi et al., 1995), also referred to as level set deformable models, represent the surface implicitly as the zero level-set of a higher-dimensional function. Geometric models have been used to constrain the distance between the exterior cortical surface (CSF-GM boundary) and the interior cortical surface (GM-WM boundary) (Zeng et al., 1999; Wang et al., 2011). Deformable models are commonly used for segmentation of a single structure, where prior knowledge of shape is important for the segmentation e.g. segmentation of the brain (specific shape) or cortical ribbon (specific thickness). Geometric models have been proposed in Dittrich et al. (2011); Wang et al. (2011); Shi et al. (2012) and parametric models in Yamaguchi et al. (2010); Gholipour et al. (2012); Kobashi and Udupa (2013) for neonatal and fetal brain and tissue segmentation.

7. Fetal segmentation

In this section we present previous studies in the literature employed for fetal segmentation. Section 7.1 presents methods for the segmentation of the brain and Section 7.2 for the segmentation into different tissue types.

7.1. Brain segmentation

Brain extraction removes the scalp and skull from the MR images and includes the CSF and brain tissues, typically for further processing. Brain segmentation from fetuses is a challenging task as the brain needs to be further separated from the maternal tissue. Additionally, considerable motion is also present that significantly complicates the task.

7.1.1. Parametric techniques

Anquez et al. (2009) adopted a three-stage process for skull segmentation. They initialy detect the eyes of the fetus with template matching and contrast, morphological and biometrical prior information. Afterwards they segment the brain in the mid-sagittal plane. A shape is finally registered to the volume and used to segment the 3D brain. Segmentation is performed with graph-cuts. Registration of a single shape may be problematic if the method is adopted in wide age ranges of the fetal brain and is prone to errors in case of motion-corrupted images.

7.1.2. Classification techniques

Ison et al. (2012) used a random forest classifier to suppress the influence of maternal tissues and identify possible locations of the brain based on 3D Haar descriptors. The brain was consequently segmented using a high-order MRF. Keraudren et al. (2014) developed a pipeline for brain detection from motion-corrupted 3D volumes. Maximally Stable Extremal Regions (MSER), regions with homogeneous intensity on the inside and high intensity differences at their boundary, are initialy detected. Scale-Invariant Feature Transform (SIFT) features are then computed for these regions, are clustered using a k-means algorithm, and then classified into brain/non-brain with a Support Vector Machine (SVM) classifier. This initial segmentation is then refined with a Random Forest classifier applied on patches of the 2D slices, and with use of a Conditional Random Field (CRF). Kainz et al. (2014) followed a similar methodology but trained a random forest classifier on 3D Gabor descriptors. The segmentation was consequently refined using a 2D level-set. The method has been implemented for GPU and requires only 7 s for the segmentation of the brain. Rajchl et al. (2016) recently proposed a method based on a 3D convolutional neural network and a CRF. The CNN and CRF are iteratively computed until convergence. Their method was trained to perform brain segmentation using a library of bounding boxes of the brain rather than manual segmentations of the whole brain volume. The presented classification methods (Ison et al., 2012; Keraudren et al., 2014; Kainz et al., 2014; Rajchl et al., 2016) have been specifically designed to deal with motion artifacts of the fetal brain MRI.

7.1.3. Atlas fusion techniques

Wright et al. (2014) employed the patch-based brain segmentation of Eskildsen et al. (2012) to extract the brain from fetal MR images. Eskildsen et al. (2012) method is a multi-resolution extension of the patch-based technique of Coupé et al. (2011) for the brain extraction from adult MRI. Multi-atlas segmentation was also used by Tourbier et al. (2015). They applied multi-atlas fusion with global weighting based on the normalized correlation coefficient (NCC). Atlas fusion techniques are sensitive to mis-registration errors that are expected in motion-corrupted fetal images. To alleviate this problem, Wright et al. (2014); Tourbier et al. (2015) employ SVR techniques prior to brain extraction.

7.2. Tissue segmentation

A few techniques have been also presented for the segmentation of the different tissue types of the fetal brain and are discussed in this section. Tissue segmentation for the fetal brain has been performed on images that have been reconstructed with SVR or that do not have evident motion.

7.2.1. Parametric techniques

Habas et al. (2008, 2010b) was the first to propose a method for fetal tissue segmentation. An EM model with bias correction was used similar to Van Leemput et al. (1999). A MRF penalty was further introduced to ensure similar labelling of nearby voxels. In their later work, Habas et al. (2009), they extended the model by combining the atlas priors with laminar priors, depth-based priors estimated using the Laplace's equation (Jones et al., 2000). Cuadra et al. (2009) proposed an EM scheme for atlas-free tissue segmentation. They used a mixture of two Gaussians for the CGM and WM instead of a single class. The Gaussian parameters of the GMM were initialized with empirical values. This may be problematic for fetal segmentation at different ages due to differences in development and myelination. They further presented a MRF with a local component, based on the voxel neighborhood, and a global component, based on the cortical distance map. PV correction is performed with knowledge-based rules. Limited evaluation was performed on four subjects. Wright et al. (2014) similarly utilised the EM-MRF segmentation method developed by Ledig et al. (2012) for the neonatal images (presented in the next section) in order to segment the tissues from fetal MRI.

7.2.2. Deformable models

Dittrich et al. (2011) presented a level-set group-wise segmentation technique where a latent atlas is inferred from the images of the database, which in turn constrains the individual segmentations. They model the segmentation with a probabilistic formulation of level-sets that incorporates an image likelihood term, a spatial prior term and a smoothness constraint. The parameters of each term are minimized in an interleaved manner. The parameters of the image likelihood term are modelled with a GMM that is optimised with the EM algorithm for each image. The spatial term parameters are estimated as an age-weighted probabilistic average of all the individual segmentations and can be thought as a 'spatio-temporal latent atlas'. All the images are aligned before the segmentation with a group-wise registration technique. The segmentation is performed for a single structure and is based on a single manually segmented atlas. Gholipour et al. (2012) proposed a shape-based segmentation technique for the segmentation of the ventricles in fetal MRI. An initial segmentation is obtained with the use of STAPLE (Warfield et al., 2004). The segmentation is then derived with a probabilistic shape segmentation that incorporates intensity and local spatial information. Penalty terms are introduced to account for the intersection of the different shapes and smoothness of the regions.

8. Neonatal segmentation

Segmentation methods have been more widely employed for the neonatal brain. Section 8.1 presents methods for brain segmentation, Section 8.2 methods for tissue segmentation and Section 8.3 methods for more detailed structural segmentation.

8.1. Brain segmentation

Brain extraction techniques used for the adult brain, such as BET (Smith, 2002) and BSE (Shattuck et al., 2001), are often successful for the neonatal brain and have been used in the literature (Anbeek et al., 2008; Srhoj-Egekher et al., 2012; Ledig et al., 2012; Makropoulos et al., 2012b; Moeskops et al., 2015; Beare et al., 2016). However, neonatal-specific brain extraction methods have been also developed and are presented in the following. The majority of the developed techniques compare their accuracy with BET and BSE.

8.1.1. Unsupervised classification techniques

Péporté et al. (2011) developed an atlas-free segmentation method based on a combination of morphological operations, region growing and edge detection to extract the brain region. Adaptive thresholding is performed with a threshold derived using k-means clustering on each 2D slice separately. Quantitative evaluation in Péporté et al. (2011) was only performed over five subjects.

8.1.2. Parametric techniques

Mahapatra (2012) proposed a skull-stripping method based on graph-cuts. They incorporate prior information from a probabilistic mask and include a smoothness term utilising gradient information.

8.1.3. Classification techniques

Serag et al. (2016) developed a method that performs classification of the MRI into brain and non-brain region using either a Naive Bayes or a Linear Discriminant Analysis classifier. Atlas selection is performed to identify atlases that provide complementary information across an atlas database. Serag et al. (2016) have compared their method with eleven other brain segmentation techniques, including BET and BSE.

8.1.4. Deformable models

Yamaguchi et al. (2010) proposed a skull-stripping method based on an active surface model. The intensity is modelled with a Gaussian Mixture Model within a Bayesian classification scheme. Prior information is incorporated from tissue probability maps of a constructed atlas. Yamaguchi et al. (2010) did not perform quantitative validation of their method and relied on visual inspection of the results. Similarly, Kobashi and Udupa (2013) presented a technique based on the Fuzzy Object Model, an active surface model using a prior shape model. Kobashi and Udupa (2013) quantitatively assess their results on 10 subjects, however do not compare their method with other brain extraction techniques. Yamaguchi et al. (2010) and Kobashi and Udupa (2013) additionally separate the CSF from the brain tissue. Shi et al. (2012) developed a meta-algorithm that combines two brain extraction techniques, BET and BSE. Parameters of the two techniques are optimised and are then used

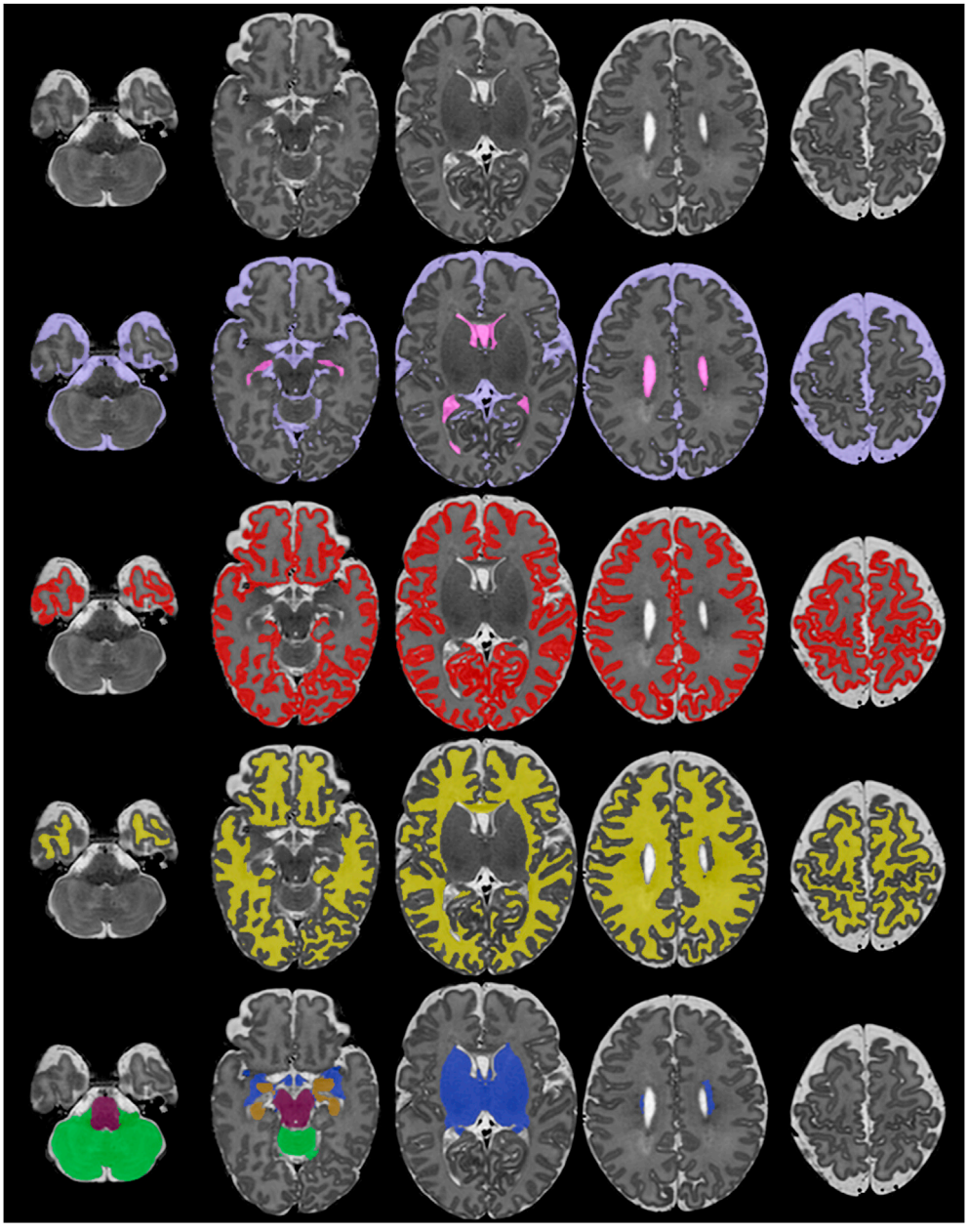

Fig. 7. Example tissue segmentation of a neonatal MRI using Draw-EM.

for the segmentation of the test subject. Brain extraction using different parameters are fused and refined with a level-set based segmentation algorithm. To reduce computation complexity, Shi et al. (2012) perform atlas selection based on the intensity similarity of the atlases with the affinity propagation technique. They perform validation over an extensive database of 246 subjects including 75 neonates and compare their technique with six other methods, including BET, BSE and STAPLE.

8.2. Tissue segmentation

Studies in the neonatal segmentation field are majorly focused to tissue segmentation of the brain MR images. This section presents methods used in the literature for the neonatal tissue segmentation. An example segmentation into different tissue types is presented in Fig. 7.

8.2.1. Unsupervised classification techniques

Gui et al. (2012a,b) proposed an atlas-free segmentation method that is based on prior knowledge about brain morphology. In their work, Gui et al. (2012b) use both the T1 and T2 modalities and segment the brain tissues with application of the watershed segmentation, region growing, active contour segmentation and morphological operations. Since Gui et al. (2012b) do not depend on atlases, their method is not affected by errors on atlas registration.

8.2.2. Parametric techniques

Prastawa et al. (2005) developed a method for tissue segmentation based on the EM algorithm of Van Leemput et al. (1999). Novelties of the work include the differentiation between the myelinated and unmyelinated WM class according to a graph based clustering technique (minimum spanning tree) and removal of outliers with the use of the Minimum Covariance Determinant (MCD) estimator. Sample locations of high atlas probability were used to estimate the initial intensity estimates with the MCD estimator. The segmentation was further refined with the use of non-parametric kernel density estimates. A drawback of the technique is that the atlas was created by averaging semi-automatic segmentations from three subjects and therefore is hard to capture the large differences undergoing in the neonatal population. Xue et al. (2007) similarly implemented an EM scheme with a MRF regularization term. However, Xue et al. (2007) abstained from using atlases for the tissue priors and instead relied on *k*-means clustering to obtain subject-specific tissue priors. Deep grey matter tissues were removed prior to processing based on manually segmented atlases. Xue et al. (2007) addressed the CSF-WM partial volume problem with a knowledge-based method implemented with connected component labelling. The authors also introduced a local splitting of the brain into different regions and estimated the Gaussian parameters in a localised fashion. An alternative approach to account for mis-registration of the atlases was proposed by Cardoso et al. (2011, 2011, 2013) proposed an EM-MRF scheme that adapts the atlas priors similar to Shiee et al. (2011). The atlas priors provided by atlases were modelled as samples drawn from a Dirichlet distribution and were adapted according to the posteriors of each EM iteration. The CSF-WM PV was modelled as mixed distributions among the different tissues. Moreover, they deviated from the classic Gaussian modelling by introducing a semi-conjugate Gaussian prior over the tissue Gaussian means initialized by manually selected patches representative for the different tissues. Melbourne et al. (2012) extended Cardoso et al. (2011, 2013) to further perform outlier rejection of intensity clusters that have a large Mahalanobis distance from the estimated model in order to reduce their influence in the parameter estimation. Makropoulos et al. (2012b) presented a segmentation method with atlas adaptivity similar to Cardoso et al. (2011, 2013). Partial volume correction for the CSF-WM intensity overlap was implemented as in Xue et al. (2007). A second partial volume correction step was added for the correction of the WM-GM boundary, which enabled a more detailed delineation of the cortical ribbon. Structure priors were obtained as a combination of atlas priors and subject-specific priors derived from intensity clustering with *k*-means to provide a better initial estimate of the priors. Ledig et al. (2012) extended the EM-MRF model of Cardoso et al. (2011, 2013) by introducing a second-order MRF in addition to the MRF model of Cardoso et al. (2011). The second-order MRF penalises the presence of a class if a pair of classes exists in the neighborhood of the class. Shi et al. (2010) presented a framework for neonatal tissue segmentation taking advantage of a subject-specific probabilistic atlas that is generated from longitudinal data acquired at a later time. The atlas is build with AFCM, a fuzzy clustering technique. Afterwards, the atlas is used in a joint registration-segmentation framework that performs atlas registration, bias field correction, and atlas-based tissue segmentation iteratively in a modified EM algorithm. In their later work (Shi et al., 2011a), the segmentations of neonatal brains computed from Shi et al. (2010) are used to construct a subject specific atlas according to their similarity to the underlying subject. The similarity is measured across a cortical GM confidence map of the subject generated with the use of a Hessian filter. The constructed subject-specific atlas is used for the segmentation of the images in a joint registration-segmentation fashion as in Shi et al. (2010). Since it is a longitudinal framework, the method by Shi et al. (2010) requires consequent imaging data of the neonatal brain. Liu et al. (2016) investigated the use of patch-based priors in an EM framework. They initially derive a subject-specific atlas with a template and tissue probabilities similarly to Habas et al. (2010b). Additional tissue probabilities are defined with a patch-based search over the subject-specific atlas. These two probabilities are fused spatially with a patch contribution metric, focusing on the intensity structure within a patch and its neighborhood, and a voxel label accuracy metric, computed based on cross-validation. They further investigated the effect of varying searching window in the patch-based search based on the local variability of the atlas.

Adaptations of adult brain segmentation software have also been proposed in the literature. Wang et al. (2012c) adapted the Statistical Parametric Mapping (SPM) Segment software for the neonatal brain segmentation. The SPM segmentation algorithm iteratively refines the tissue segmentation, bias correction and non-linear registration of a probabilistic atlas. The tissue segmentation method was based on an EM scheme and the joint cost function was optimised with ICM. After convergence, partial volume correction was performed with the use of connected component labelling. Wu and Avants (2012) presented a technique based on the Atropos tool (Avants et al., 2011). An EM-MRF technique was used with ICM parameter optimisation. Both T1 and T2 images were used in a multivariate data-term. Clusters of misclassified voxels were corrected based on the atlas-based prior probabilities. Beare et al. (2016) extended the segmentation method implemented in SPM for the neonatal brain with the use of morphological operations, watershed transform and reconstruction by dilation.

8.2.3. Classification techniques

Anbeek et al. (2008, 2013) proposed a tissue segmentation method based on *k*-NN classification. They construct a multidimensional feature space based on intensity and spatial features of training images. The segmentation is estimated from the affinity of the *k* closest neighbors in the multidimensional space for each voxel of the unseen image. In Anbeek et al. (2008) they compute the spatial features directly from the coordinates of the image. In their later work, Anbeek et al. (2013), they improve the definition of the spatial features by using the spatial coordinates of an average brain image. Srhoj-Egekher et al. (2012) proposed a method based on label fusion and supervised classification. The priors of an initial label fusion step are combined with the probabilities from an independent 2-class *k*-NN classification for each tissue. The *k*-NN classification is performed on intensity features derived from both T1 and T2 modalities. A final step is using a naive Bayes classifier in a reduced dimensional space obtained with Principal Component Analysis to classify voxels assigned to more than one tissue classes. Chiţă et al. (2013); Moeskops et al. (2015) presented a multi-stage supervised classification technique for the neonatal image segmentation. Voxel classification was

performed in three stages: The feature space of the algorithm was composed of spatial, intensity features and the current probabilistic output. Intensity features were obtained from the T2 images in Moeskops et al. (2015) and both T1 and T2 images in Chiţă et al. (2013). The first and second stage perform independent 2-class classification for each tissue separately and the third stage uses a 4-class classification for all the classes. Chiţă et al. (2013) used a *k*-NN classifier for all the stages. Moeskops et al. (2015) used a *k*-NN classifier for the first and third stage and a SVM classifier for the second stage. The best features of each stage were selected using a forward feature selection scheme. Similarly to Chiţă et al. (2013), Wang et al. (2015) used a classification scheme on multiple stages based on intensity features and the current probabilistic output. Using this scheme, they estimate the probability maps which are consequently refined with sparse representation. Random forests were used for the classification and were trained on T1, T2 and FA images. More recently, Moeskops et al. (2016) utilised a multi-scale CNN for the segmentation of the brain tissues. 2D patches are used across the acquisition plane. Multiple patch and kernel sizes are combined in the output layer to result in the final segmentation. Sanroma et al. (2016) formulated the segmentation problem as a combination of methods in an ensemble. They combined two methods, joint label fusion based on Wang et al. (2012a) and an intensity-based method with an SVM trained on super-voxels of a template image. They then learn regional weighting of the two methods in an ensemble method based on the predictions and probabilistic estimates of the two methods. Classification techniques have presented highly accurate results on a neonatal tissue segmentation challenge, NeoBrainS12 (presented in more detail in Section 9.1). They are however more sensitive than parametric and unsupervised techniques to differentiations in brain intensities.

8.2.4. Atlas fusion techniques

Weisenfeld et al. (2006); Weisenfeld and Warfield (2009) used an iterative sample editing process for segmentation of the brain tissues. Initially, the labels of the atlases were fused into the subject space to result in an initial estimate of the segmentation. Afterwards, they iteratively refine each atlas' samples with the use of the segmentation, and reestimate the segmentation with the STAPLE algorithm. They model spatial homogeneity with a MRF term. Weisenfeld and Warfield (2009) further perform CSF-WM PV correction with a method similar to Xue et al. (2007). The tissue segmentation of Weisenfeld and Warfield (2009) requires an accurate alignment of atlases, which is a non-trivial problem due to the large developmental changes of the neonatal brain. Kim et al. (2015) developed a pipeline that performs segmentation and surface reconstruction of the neonatal brain. Segmentation is performed with a technique combining the patch-based model of Coupé et al. (2011) and the joint atlas error estimation of Wang et al. (2012a). Similar patches from the atlases are fused with a weighting accounting for joint atlas errors based on Wang et al. (2012a). Kim et al. (2015) segment the brain into two parts, the cortical ribbon and the remaining brain area as a whole.

8.2.5. Deformable models

Wang et al. (2011) proposed a segmentation algorithm based on coupled level sets with a local intensity information term, atlas tissue priors and a cortical thickness constraint. Local intensity information was modelled with Gaussian distributions with spatially varying mean and variance. The cortical thickness constraint is used to retain the CSF/GM and GM/WM surface distance within a predefined extent. CSF-WM PV correction is incorporated in the model with a method similar to Xue et al. (2007). They later (Wang et al., 2012b) extended their method in a multi-modal and longitudinal framework. The segmentation utilised a multi-modality data fitting term using both T1, T2 and FA images. Additionally, images obtained at different timepoints were incorporated in a longitudinally guided level-set segmentation. The different timepoints were iteratively co-registered with a 4D registration method and segmented in a longitudinal fashion with constraints from neighboring timepoints. Wang et al. (2014) proposed the use of a spatially-consistent subject-specific atlas for the segmentation built with patch-based sparse representation. Wang et al. (2011, 2012b, 2014) focus on the differentiation between the WM, GM and CSF and don't separate the deep GM from the cortical GM or segment the brainstem and cerebellum.

8.3. Structural segmentation

Delineation of more localised structures of the brain is limited. Due to the lack of detailed manually segmented atlases, early methods (Peterson et al., 2003; Haidar et al., 2005; Mewes et al., 2006; Gilmore et al., 2007; Thompson et al., 2007) adopted a parcellation of the CGM and WM regions based on manually placed axis on the brain. These axis divided the CGM/WM into 16 parts: frontal, precentral, central and occipital regions divided into superior and inferior part for the left and right hemisphere. The first regional atlases of the brain were manually delineated by Oishi et al. (2011); Gousias et al. (2012). Segmentation methods have used these atlases or propagated labels from adult atlases to delineate regional structures of the brain. Propagation of adult brain structures may be problematic as the different structures of the brain may have not been yet formed in the developing brain. An example segmentation into different tissue types is presented in Fig. 8.

8.3.1. Parametric techniques

Makropoulos et al. (2012a, 2014) utilised the atlases by Gousias et al. (2012) to automatically segment the neonatal brain into 87 regions with an EM method similar to Makropoulos et al. (2012b). In Makropoulos et al. (2014) they combine the EM method with weighted label fusion according to the local intensity gradient in the MR image. Makropoulos et al. (2016) extended the method proposed in Makropoulos et al. (2014) with a more detailed delination of the cortical ribbon using thickness-based correction and PV correction of the WM-CGM boundary. Makropoulos et al. (2014) perform segmentation on different ages of the neonatal brain from early preterm to term age. However, due to limited manual delination, quantitative evaluation on early preterm brain is presented for a few brain structures. Wu et al. (2014) propagated labels from 20 adult OASIS templates. After an initial tissue segmentation based on EM, they parcellate the cortical ribbon into 62 regions with the label fusion method proposed by Wang et al. (2012a).

8.3.2. Atlas fusion techniques

Gousias et al. (2013) utilised their manually segmented atlases (Gousias et al. (2012)) and investigated the segmentation based on label fusion of the atlases or alignment of a maximum probability atlas. Label fusion requires accurate registration of the atlases, which is difficult between different ages of the neonatal brain.

9. Segmentation evaluation

The accuracy of segmentation methods is quantitatively assessed with respect to manual annotations which are used as the ‘gold standard'. The accuracy is typically estimated with overlap measures and/or surface-distance measures. The most common overlap metric used in the fetal and neonatal literature is the Dice coefficient. The Dice coefficient (Dice, 1945) between two segmentations S_a and S_m, of the same object, is defined as

$$Dice = \frac{2|S_a \cap S_m|}{|S_a| + |S_m|} \quad (1)$$

where $|S_a|$, $|S_m|$ is the number of voxels of the segmented object in S_a and S_m respectively and $|S_a \cap S_m|$ the number of common voxels between the two segmentations. The measure takes a value of 1 in the case of perfect match amongst the two segmentations and 0 when there is no overlap.

Surface-based distance measures are sometimes reported (Mahapatra, 2012; Moeskops et al., 2015; Išgum et al., 2015; Serag et al., 2016). The

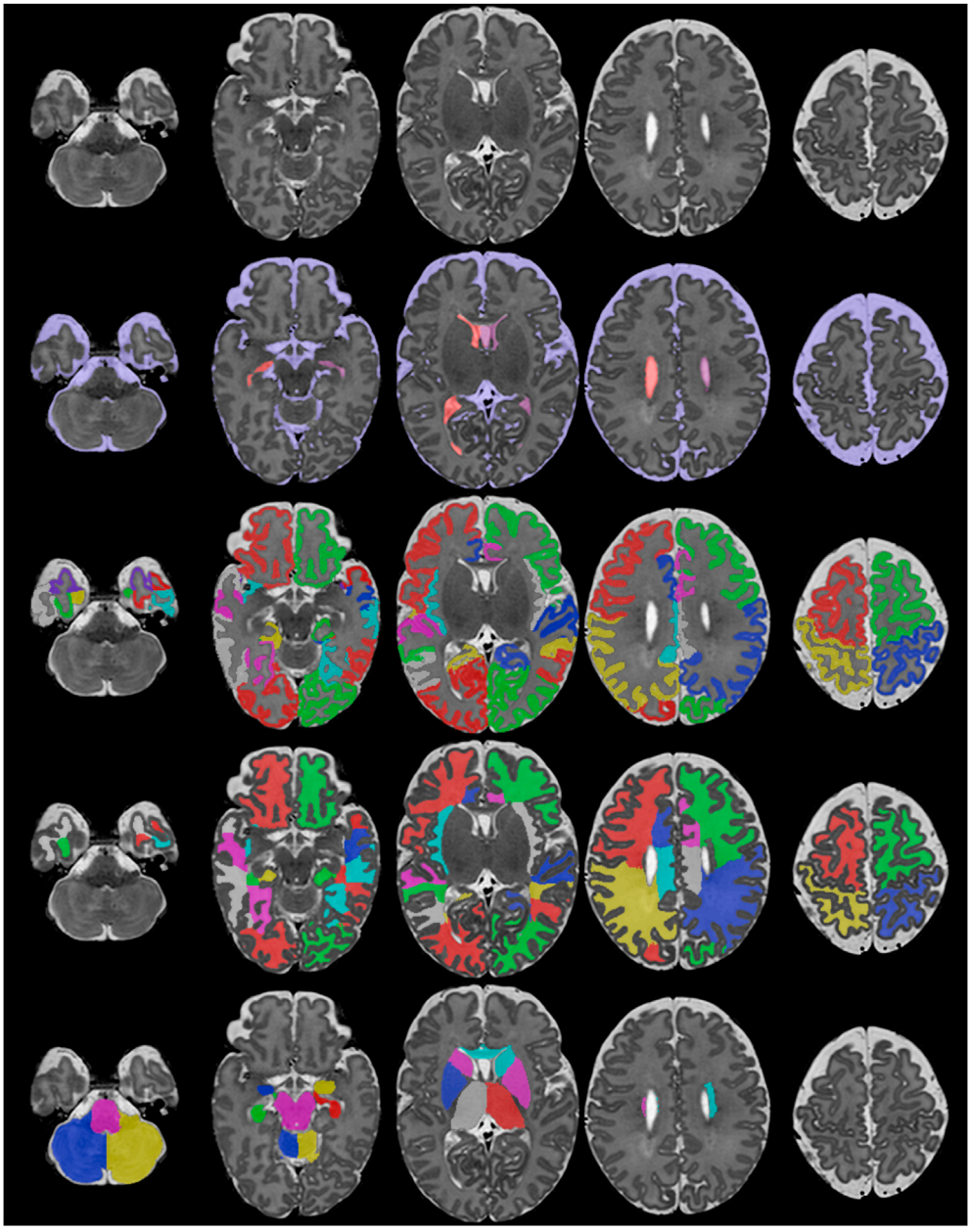

Fig. 8. Example structural segmentation of a neonatal MRI using Draw-EM.

mean surface distance between a surface $S\prime_a$ and $S\prime_m$, computed from the segmentations S_a and S_m respectively, is defined as the mean distance between corresponding, e.g. closest, points of the two surfaces. Accordingly, the Hausdorff distance is computed as the maximum distance between corresponding points of the two surfaces.

Due to the limited amount of manually annotated data and the rapid developmental differences occurring in the perinatal domain, quantitative evaluation is relatively limited. Manually segmented atlases used as training data are usually employed in a cross-validation fashion to compare the automatic performance versus that of the human rater. Additionally, quantitative evaluation is sometimes complemented by comparison with manually parcellated data that are not used for the training of the algorithms. These data may be labelled on their entirety (e.g. Wang et al. (2011, 2014); Beare et al. (2016)) or partially on selected slices and/or structures (e.g. Weisenfeld et al. (2006); Moeskops et al. (2015)). Direct comparison of segmentation techniques is not easily feasible due to different data acquisition parameters, different manual reference segmentations as well as different definition of structures and number of structures segmented. To address this problem and provide the community with current state-of-the-art results, a neonatal tissue segmentation challenge, NeoBrainS12, was organised at MICCAI 2012 by Išgum et al. (2015). The challenge is briefly introduced in the following section.

9.1. NeoBrainS12

A recent neonatal brain segmentation challenge, NeoBrainS12 (Išgum et al., 2015), was held and aimed to evaluate the performance of submitted neonatal tissue segmentation algorithms on a common reference. Three different sets of T1 and T2 images were provided as part of the NeoBrainS12 challenge: axial scans acquired at 40 weeks corrected age (Set 1), coronal scans acquired at 30 weeks corrected age (Set 2) and coronal scans acquired 40 weeks corrected age (Set 3). Imaging data of seven infants were included from Set 1 and Set 2 and five infants from Set 3. The brain MR images were manually parcellated in eight regions: cortical grey matter (CGM), unmyelinated white matter (WM),

myelinated white matter (MWM), brainstem, basal ganglia and thalami (BGT), cerebellum, CSF and ventricles. The segmentation protocol is described in the webpage of the challenge, http://neobrains12.isi.uu.nl. The challenge consisted of two stages: a part prior to the challenge and an on-site part. Datasets of three infants per set were provided as test data in the part prior to the challenge and two infants per set at the on-site part, without the manual segmentations. The algorithms were evaluated on these datasets. The teams could select which datasets and tissue types to segment. A two hours timeframe was set for the on-site part. The remaining datasets of two infants per Set 1 and Set 2 were provided as training data accompanied by the manual segmentations.

The following methods, detailed in Section 8.2, were submitted to the challenge: Makropoulos et al. (2012b), Wang et al. (2012c), Melbourne et al. (2012), Wu and Avants (2012), Gui et al. (2012a), Srhoj-Egekher et al. (2012), Anbeek et al. (2008), Chiță et al. (2013). Example segmentations with different techniques submitted to the challenge are presented in Fig. 9.

The segmentation accuracy was assessed separately for the on-site part and the part prior to the challenge. Table 4 presents the overlap, measured with the Dice coefficient, between the submitted automatic techniques and the manual segmentations. It should be noted here that NeoBrainS12 is still open for method submission and is an important resource for benchmarking purposes. Since the end of the NeoBrainS12 challenge, a growing number of studies have evaluated their technique on the challenge data (Moeskops et al., 2015; Wang et al., 2015; Beare et al., 2016; Moeskops et al., 2016; Sanroma et al., 2016). Accurate segmentation results were presented by all the methods in the challenge with best Dice overlaps for the different tissues ranging from 0.71 to 0.95.

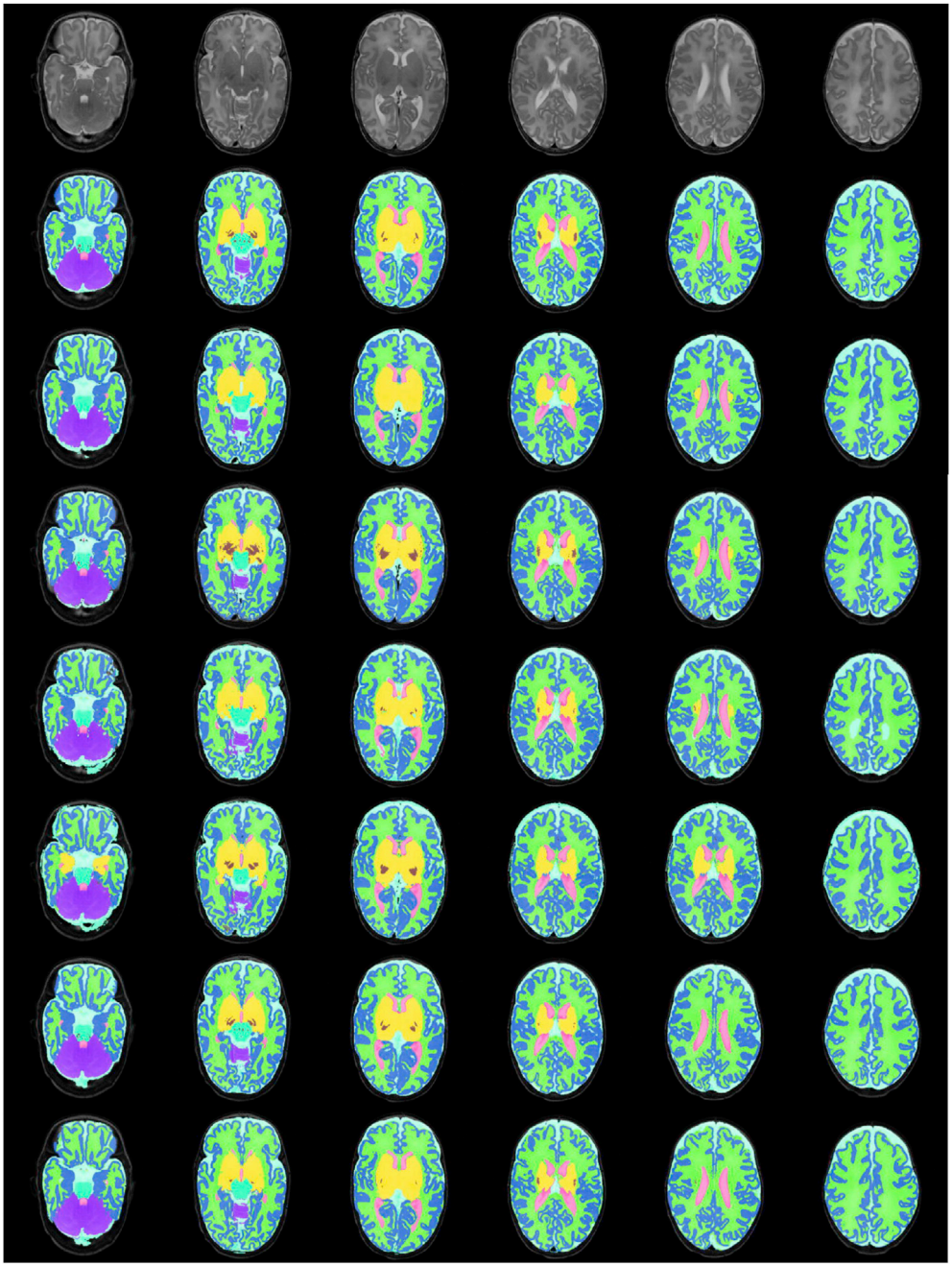

Fig. 9. Example tissue segmentations of a neonatal brain MRI from Set 1 with different techniques submitted to the NeoBrainS12 challenge (image copied from Išgum et al. (2015)). From top to bottom: MR image, manual segmentation, Makropoulos et al. (2012b), Wang et al. (2012c), Melbourne et al. (2012), Wu and Avants (2012), Srhoj-Egekher et al. (2012), Anbeek et al. (2008).

Table 4
Results of the web-based and on-site part of the NeoBrainS12 challenge (data from http://neobrains12.isi.uu.nl). The submitted algorithms are compared in terms of the Dice coefficient with the manual reference. Methods noted with * had the manual reference data of the test set available during the method construction and were not included in the method ranking in NeoBrainS12. The best result for each tissue is noted with bold font.

	CGM			WM			MWM			WM+MWM			CSF		
	Set 1	Set 2	Set 3	Set 1	Set 2	Set 3	Set 1	Set 2	Set 3	Set 1	Set 2	Set 3	Set 1	Set 2	Set 3
Web-based results															
Makropoulos et al. (2012b)	0.84	0.70	0.75	0.89	0.91	0.86	–	–	–	–	–	–	0.76	0.84	**0.75**
Wang et al. (2012c)	0.83	0.60	0.72	0.88	0.86	**0.84**	0.43	0.29	**0.52**	0.88	0.86	0.84	0.72	0.75	0.71
Melbourne et al. (2012)	0.83	**0.71**	0.73	0.87	0.90	0.84	0.22	0.16	0.08	0.87	**0.90**	0.83	0.71	0.76	0.58
Wu and Avants (2012)	0.80	0.60	0.69	0.85	0.87	0.83	0.32	**0.69**	0.07	0.84	0.87	0.82	0.61	0.63	0.71
Gui et al. (2012a)	–	–	**0.76**	–	–	**0.89**	–	–	–	–	–	–	–	–	
Srhoj-Egekher et al. (2012)*	**0.85**	–	–	**0.91**	–	–	**0.55**	–	–	**0.91**	–	–	**0.77**	–	–
Anbeek et al. (2008)*	0.82	–	–	0.87	–	–	0.46	–	–	0.87	–	–	0.72	–	–
Chiţă et al. (2013)*	–	0.70	–	–	**0.94**	–	–	–	–	–	–	–	–	**0.85**	–
	ventricles			CSF+ventricles			brainstem			cerebellum			BGT		
	Set 1	Set 2	Set 3	Set 1	Set 2	Set 3	Set 1	Set 2	Set 3	Set 1	Set 2	Set 3	Set 1	Set 2	Set 3
Makropoulos et al. (2012b)	0.80	0.86	0.82	0.77	**0.85**	**0.77**	0.84	**0.75**	**0.73**	0.91	**0.87**	**0.92**	0.91	0.82	0.86
Wang et al. (2012c)	0.85	**0.88**	0.83	0.74	0.78	0.72	0.80	0.69	0.71	0.92	**0.87**	0.90	0.87	0.82	**0.88**
Melbourne et al. (2012)	0.81	0.86	0.70	0.73	0.78	0.61	0.82	0.73	**0.73**	0.90	**0.87**	**0.92**	0.89	**0.84**	0.85
Wu and Avants (2012)	**0.86**	0.87	**0.84**	0.64	0.66	0.72	0.74	0.65	0.36	0.91	0.85	0.91	0.80	0.74	0.79
Gui et al. (2012a)	–	–	–	–	–	0.71	–	–	0.71	–	–	0.89	–	–	0.85
Srhoj-Egekher et al. (2012)*	0.83	–	–	**0.78**	–	–	**0.87**	–	–	**0.93**	–	–	**0.93**	–	–
Anbeek et al. (2008)*	0.81	–	–	0.73	–	–	0.85	–	–	**0.93**	–	–	0.92	–	–
Chiţă et al. (2013)*	–	–	–	–	–	–	–	–	–	–	–	–	–	–	–
On-site results															
Makropoulos et al. (2012b)	**0.88**	0.67	0.74	0.91	0.91	0.86	–	–	–	–	–	–	0.82	0.82	**0.81**
Wang et al. (2012c)	0.86	0.54	0.71	0.89	0.85	0.85	0.55	**0.21**	**0.42**	0.89	**0.71**	**0.84**	0.81	0.72	0.78
Melbourne et al. (2012)	–	–	–	–	–	–	–	–	–	–	–	–	–	–	–
Wu and Avants (2012)	–	–	–	–	–	–	–	–	–	–	–	–	–	–	–
Gui et al. (2012a)	–	–	**0.76**	–	–	**0.89**	–	–	–	–	–	–	–	–	–
Srhoj-Egekher et al. (2012)*	**0.88**	–	–	**0.92**	–	–	**0.68**	–	–	**0.92**	–	–	**0.85**	–	–
Anbeek et al. (2008)*	0.86	–	–	0.88	–	–	0.62	–	–	0.88	–	–	0.81	–	–
Chiţă et al. (2013)*	–	**0.73**	–	–	**0.94**	–	–	–	–	–	–	–	–	**0.87**	–
	ventricles			CSF+ventricles			brainstem			cerebellum			BGT		
	Set 1	Set 2	Set 3	Set 1	Set 2	Set 3	Set 1	Set 2	Set 3	Set 1	Set 2	Set 3	Set 1	Set 2	Set 3
Makropoulos et al. (2012b)	0.84	0.80	0.80	0.83	**0.83**	**0.82**	0.82	**0.78**	**0.77**	0.93	0.88	0.90	0.90	0.82	0.88
Wang et al. (2012c)	0.86	**0.88**	**0.85**	0.82	0.75	0.79	0.76	0.73	0.72	0.93	**0.89**	0.89	0.90	**0.83**	**0.89**
Melbourne et al. (2012)	–	–	–	–	–	–	–	–	–	–	–	–	–	–	–
Wu and Avants (2012)	–	–	–	–	–	–	–	–	–	–	–	–	–	–	–
Gui et al. (2012a)	–	–	–	–	–	**0.82**	–	–	0.72	–	–	**0.93**	–	–	0.87
Srhoj-Egekher et al. (2012)*	**0.89**	–	–	**0.85**	–	–	**0.87**	–	–	**0.95**	–	–	**0.92**	–	–
Anbeek et al. (2008)*	0.84	–	–	0.82	–	–	0.86	–	–	0.94	–	–	0.91	–	–
Chiţă et al. (2013)*	–	–	–	–	–	–	–	–	–	–	–	–	–	–	–

Exception is the myelinated WM which could not be consistently segmented. Differences in the results between the submitted methods were small in most of the cases. Furthermore, since evaluation was performed on a limited number of images (two images per set on the on-site and three per set in the part prior to the challenge), significance of the results was not assessed in NeoBrainS12.

10. Future directions

The interest in perinatal segmentation is constantly increasing as more and better quality images are obtained that allow quantitative evaluation of the brain. Although segmentation techniques are quite successful and report segmentation accuracies similar to those in adult brain imaging, there are still remaining issues that need to be resolved. This section presents existing challenges and future directions for research in the perinatal field.

10.1. Atlases and availability of resources

A limiting factor in the development of automatic segmentation techniques for the perinatal brain is the lack of manually segmented atlases. The most comprehensive manually labelled atlases were introduced by Gousias et al. (2012) and more recently by Alexander et al. (2016) that defined 50 and 100 structures respectively at term-equivalent age. There are no detailed atlases for the preterm period and for the fetal brain. This is particularly of interest since the brain structures are being formed and developed during this period. Therefore methods that propagate labels from the term age to the earlier periods (Makropoulos et al., 2016) may resort to mapping of small regions rather than utilising observed anatomical variability. Manually segmented atlases at the fetal and preterm age would help to further adopt segmentation in the early brains. Furthermore, public availability of the atlases is crucial for method development from the community.

A contributing factor to the limited adoption of segmentation techniques in the neonatal and fetal domain is the lack of publically available MRI data and databases that can be used for benchmarks. NeoBrainS12 (Išgum et al., 2015) provided a limited amount of manually labelled data that can be used to assess accuracy of algorithms in the segmentation of the different tissue types. Similar segmentation competitions for more detailed structures of the neonatal brain as well as the fetal brain would allow to quantitatively elucidate differences between segmentation techniques. Additionally, access to larger amount of even unlabelled data could potentially help increase the performance of semi-supervised methods. Limited data are utilised in the majority of segmentation techniques and this is partly due to limited amount of publically available resources. dHCP,[2] an ongoing project that aims to study the connectome of the developing brain, will provide the research community with large amounts of structural and diffusion data. Similar recourses are needed to

create large databases of subjects that can be used for method development. Finally, open-source segmentation software will allow faster development of tools and collaboration between universities as well as comparisons between methods.

10.2. Segmentation of myelinated WM

Differentiation between myelinated and unmyelinated white matter is of major significance. Myelin content is progressively increased in the neonatal brain and allows for faster signal conductivity in the brain. As such it is assumed to have correlates to the functional maturation of brain (van der Knaap et al., 1991). Preterm brains have been associated with reduced myelination compared to their term peers (Hüppi et al., 1996). Only a few studies have attempted to make a differentiation between myelinated and unmyelinated white matter (Prastawa et al., 2005; Wang et al., 2012c; Melbourne et al., 2012; Wu and Avants, 2012; Srhoj-Egekher et al., 2012; Anbeek et al., 2008) with the majority of them using the myelinated WM definitions of the NeoBrainS12 challenge. This problem could be further linked to the lack of manually segmented atlases defining these regions, however unsupervised techniques may be able to additionally aid such a differentiation.

10.3. Segmentation methodology

With respect to segmentation methodology, there are opportunities for state-of-the-art techniques to improve the current segmentation accuracy. Deep learning and convolutional neural networks are extremely popular in the computer vision domain. They have provided large improvements in challenging computer vision problems (Krizhevsky et al., 2012) and more recently medical imaging problems (de Brebisson and Montana, 2015; Zhang et al., 2015; Kamnitsas et al., 2016; Nie et al., 2016). In the perinatal segmentation domain, CNNs have only be used in Moeskops et al. (2016); Rajchl et al. (2016). Semi-supervised techniques have been also rarely adopted (Dittrich et al., 2011). Studies in the adult brain (Wolz et al., 2010) have demonstrated an increase in segmentation accuracy with introduction of unlabelled data in the segmentation process. Another important direction for method development is the implementation of robust methods in presence of pathologies. Abnormalities in the brain, which are common in the fetal and neonatal period, such as ventriculomegaly or hypoxic-ischemic encephalopathy can significantly affect the performance of developed techniques.

10.4. Automated segmentation quality control

Automatic segmentation methods can not be completely accurate all the time. An important research direction is to provide certainty estimates directly from the methods for each segmented case. Alternatively post-hoc solutions could be developed to automatically rate the segmentation quality of a method e.g. based on the consistency across different cases. This will allow to identify problems of segmentation methods and identify inaccurate cases in large clinical studies.

10.5. Application in clinical studies

The most important goal of segmentation is to aid in the detection and characterization of neonatal and fetal pathologies. Quantitative measurements derived using segmentation techniques have the potential to improve understanding of major pathologies in the neonatal brain, such as hypoxic-ischemic encephalopathy, cerebral infarction, periventricular leukomalacia, hemorrhages and lesions (Rutherford, 2002), and the fetal brain, such as ventriculomegaly, agenesis of the corpus callosum, malformations of cortical development and posterior fossa anomalies (Weisstanner et al., 2015). Only limited studies have been published with quantitative measurements in such abnormalities e.g. Ball et al. (2010); Bassi et al. (2011); Keunen et al. (2012); Tusor et al. (2012); Kyriakopoulou et al. (2014); Lockwood Estrin et al. (2016); Kersbergen et al. (2016); Murphy et al. (2017). Utilisation of segmentation techniques to obtain quantitative volumetric measures of the normal developing brain and different pathologies is essential to define normality centiles and identify markers of abnormality. A publically available resource describing volumes obtained from large databases would be useful as a reference for clinical studies and could potentially promote the use of automatic segmentation in clinical practice. Additionally, DTI and fMRI measurements for detailed structures could be used to further extend this resource. A prerequisite though for such an analysis is the development of robust methods and quality control of developed methods.

10.6. Link of neonatal to adult period

Segmentation of detailed brain structures is further required to link the structural development from the neonatal and fetal period up to the adult period. The atlases constructed by Alexander et al. (2016) provide an important resource to create this link between the neonatal and adult age. Alexander et al. (2016) delineated cortical structures in the neonatal brain based on the Desikan-Killiany protocol (Desikan et al., 2006) that is commonly used for cortical parcellation studies in the adult brain. Furthermore, the atlases of de Macedo Rodrigues et al. (2015) parcellated 32 regions of the brain in neonates and infants up to 2 years of age that allows to link development in the infant period. Longitudinal segmentation methods such as Shi et al. (2010); Wang et al. (2012b) are important to consistently segment structures through different timepoints of development. It should be noted here that infant brain MRI acquired during the isointense phase (around 6–8 months) is particularly challenging for segmentation as the WM and CGM intensity distributions overlap significantly. There are only limited approaches that address this problem (Nie et al., 2016; Zhang et al., 2015).

11. Conclusion

Segmentation of the fetal and neonatal brain is increasingly gaining interest with the acquisition of better quality images and the increased focus on fetal and neonatal development. In this review paper we have surveyed existing techniques in the literature for the task of fetal and neonatal brain MRI segmentation. We initially introduced the challenges in the segmentation domain and more specifically for the perinatal brain. Existing atlases that are used as prior knowledge were consequently presented. This was followed by a brief description of image acquisition and image preprocessing techniques used prior to the segmentation to reduce image artifacts due to motion, noise and intensity inhomogeneity. We classified and presented the segmentation techniques according to the target population, the segmentation task and the methodology followed. We presented evaluation metrics for assessing the quality of the segmentation and described NeoBrainS12, a recent segmentation challenge, that is often used as benchmark for the neonatal tissue segmentation methods. Finally we presented remaining challenges and possible future directions in the field. There are still remaining obstacles in method development mainly due to lack of data. However with increasing availability of recourses for the perinatal brain, it is expected that these will be overcome in the near future. Future methods should be robust to the large changes of the developing brain and the presence of the pathologies. This will allow the detailed characterization of pathological cases and can potentially allow automatic segmentation to be used in clinical practice.

References

Adams, R., Bischof, L., 1994. Seeded region growing. IEEE Trans. Pattern Anal. Mach. Intell. 16 (6), 641–647.

Al-Attas, R., El-Zaart, A., 2007. Thresholding of medical images using minimum cross entropy. In: 3rd Kuala Lumpur International Conference on Biomedical Engineering 2006, pp. 296–299.

Alexander, B., Murray, A.L., Loh, W.Y., Matthews, L.G., Adamson, C., Beare, R., Chen, J., Kelly, C.E., Rees, S., Warfield, S.K., Anderson, P.J., Doyle, L.W., Spittle, A.J.,

Cheong, J.L.Y., Seal, M.L., Thompson, D.K., 2016. A new neonatal cortical and subcortical brain atlas: the Melbourne Children's Regional Infant Brain (M-CRIB) atlas. NeuroImage 147, 841–851.
Anbeek, P., Išgum, I., van Kooij, B.J.M., Mol, C.P., Kersbergen, K.J., Groenendaal, F., Viergever, M.A., de Vries, L.S., Benders, M.J.N.L., 2013. Automatic segmentation of eight tissue classes in neonatal brain MRI. PloS One 8 (12), e81895.
Anbeek, P., Vincken, K.L., Groenendaal, F., Koeman, A., van Osch, M.J.P., van der Grond, J., 2008. Probabilistic brain tissue segmentation in neonatal magnetic resonance imaging. Pediatr. Res. 63 (2), 158–163.
Anquez, J., Angelini, E.D., Bloch, I., 2009. Automatic Segmentation of Head Structures on Fetal MRI. IEEE, pp. 109–112.
Artaechevarria, X., Munoz-Barrutia, A., Ortiz-de Solorzano, C., 2009. Combination strategies in multi-atlas image segmentation: application to brain MR data. IEEE Trans. Med. Imaging 28 (8), 1266–1277.
Ashburner, J., Friston, K.J., 2005. Unified segmentation. NeuroImage 26 (3), 839–851.
Avants, B.B., Tustison, N.J., Wu, J., Cook, P.A., Gee, J.C., 2011. An open source multivariate framework for n-tissue segmentation with evaluation on public data. Neuroinformatics 9 (4), 381–400.
Ball, G., Counsell, S.J., Anjari, M., Merchant, N., Arichi, T., Doria, V., Rutherford, M.A., Edwards, A.D., Rueckert, D., Boardman, J.P., 2010. An optimised tract-based spatial statistics protocol for neonates: applications to prematurity and chronic lung disease. NeuroImage 53 (1), 94–102.
Bankman, I., 2008. Handbook of Medical Image Processing and Analysis, 2 edition. Academic Press.
Bassi, L., Chew, A., Merchant, N., Ball, G., Ramenghi, L., Boardman, J., Allsop, J.M., Doria, V., Arichi, T., Mosca, F., Edwards, A.D., Cowan, F.M., Rutherford, M.A., Counsell, S.J., 2011. Diffusion tensor imaging in preterm infants with punctate white matter lesions. Pediatr. Res. 69 (6), 561–566.
Beare, R.J., Chen, J., Kelly, C.E., Alexopoulos, D., Smyser, C.D., Rogers, C.E., Loh, W.Y., Matthews, L.G., Cheong, J.L.Y., Spittle, A.J., Anderson, P.J., Doyle, L.W., Inder, T.E., Seal, M.L., Thompson, D.K., 2016. Neonatal brain tissue classification with morphological adaptation and unified segmentation. Front. Neuroinform. 10, 12.
Belaroussi, B., Milles, J., Carme, S., Zhu, Y.M., Benoit-Cattin, H., 2006. Intensity non-uniformity correction in MRI: existing methods and their validation. Med. Image Anal. 10 (2), 234–246.
Bezdek, J.C., 1981. Pattern Recognition with Fuzzy Objective Function Algorithms. Kluwer Academic Publishers, Norwell, MA, USA.
Blesa, M., Serag, A., Wilkinson, A.G., Anblagan, D., Telford, E.J., Pataky, R., Sparrow, S.A., Macnaught, G., Semple, S.I., Bastin, M.E., Boardman, J.P., 2016. Parcellation of the healthy neonatal brain into 107 regions using atlas propagation through intermediate time points in childhood. Front. Neurosci. 10.
Boardman, J.P., Craven, C., Valappil, S., Counsell, S.J., Dyet, L.E., Rueckert, D., Aljabar, P., Rutherford, M.A., Chew, A.T.M., Allsop, J.M., Cowan, F., Edwards, A.D., 2010. A common neonatal image phenotype predicts adverse neurodevelopmental outcome in children born preterm. NeuroImage 52 (2), 409–414.
Cardoso, M.J., Melbourne, A., Kendall, G.S., Modat, M., Hagmann, C.F., Robertson, N.J., Marlow, N., Ourselin, S., 2011. Adaptive neonate brain segmentation. Med. Image Comput. Comput. Assist. Interv. (MICCAI) 14 (Pt 3), 378–386.
Cardoso, M.J., Melbourne, A., Kendall, G.S., Modat, M., Robertson, N.J., Marlow, N., Ourselin, S., 2013. AdaPT: an adaptive preterm segmentation algorithm for neonatal brain MRI. NeuroImage 65, 97–108.
Chiţă, S.M., Benders, M., Moeskops, P., Kersbergen, K.J., Viergever, M.A., Išgum, I., 2013. Automatic segmentation of the preterm neonatal brain with MRI using supervised classification. In: SPIE Medical Imaging. International Society for Optics and Photonics, vol. 8669, 86693X–86693X–6.
Christensen, G.E., Rabbitt, R.D., Miller, M.I., 1994. 3d brain mapping using a deformable neuroanatomy. Phys. Med. Biol. 39 (3), 609–618.
Collins, D.L., Holmes, C.J., Peters, T.M., Evans, A.C., 1995. Automatic 3-D model-based neuroanatomical segmentation. Hum. Brain Mapp. 3 (3), 190–208.
Cordero-Grande, L., Teixeira, R.P.A.G., Hughes, E.J., Hutter, J., Price, A.N., Hajnal, J.V., 2016. Sensitivity encoding for aligned multishot magnetic resonance reconstruction. IEEE Trans. Comput. Imaging 2 (3), 266–280.
Counsell, S.J., Edwards, A.D., Chew, A.T.M., Anjari, M., Dyet, L.E., Srinivasan, L., Boardman, J.P., Allsop, J.M., Hajnal, J.V., Rutherford, M.A., Cowan, F.M., 2008. Specific relations between neurodevelopmental abilities and white matter microstructure in children born preterm. Brain 131 (12), 3201–3208.
Counsell, S.J., Rutherford, M.A., 2002. Magnetic resonance imaging of the newborn brain. Curr. Paediatr. 12 (5), 401–413.
Coupé, P., Manjón, J.V., Fonov, V., Pruessner, J., Robles, M., Collins, D.L., 2011. Patch-based segmentation using expert priors: application to hippocampus and ventricle segmentation. NeuroImage 54 (2), 940–954.
Cuadra, M.B., Schaer, M., Guibaud, L., Eliez, S., Thiran, J.-p., 2009. Brain tissue segmentation of fetal MR images. In: MICCAI Workshop on Image Analysis for Developing Brain.
de Brebisson, A., Montana, G., 2015. Deep Neural Networks for Anatomical Brain Segmentation arXiv:1502.02445 [cs, stat].
de Macedo Rodrigues, K., Ben-Avi, E., Sliva, D.D., Choe, M.-s., Drottar, M., Wang, R., Fischl, B., Grant, P.E., Zöllei, L., 2015. A FreeSurfer-compliant consistent manual segmentation of infant brains spanning the 0-2 year age range. Front. Hum. Neurosci. 9, 21.
Delobel-Ayoub, M., Arnaud, C., White-Koning, M., Casper, C., Pierrat, V., Garel, M., Burguet, A., Roze, J.-C., Matis, J., Picaud, J.-C., Kaminski, M., Larroque, B., 2009. Behavioral problems and cognitive performance at 5 Years of age after very preterm birth: the EPIPAGE study. Pediatrics 123 (6), 1485–1492.
Desikan, R.S., Ségonne, F., Fischl, B., Quinn, B.T., Dickerson, B.C., Blacker, D., Buckner, R.L., Dale, A.M., Maguire, R.P., Hyman, B.T., Albert, M.S., Killiany, R.J., 2006. An automated labeling system for subdividing the human cerebral cortex on MRI scans into gyral based regions of interest. NeuroImage 31 (3), 968–980.
Devi, C.N., Chandrasekharan, A., Sundararaman, V.K., Alex, Z.C., 2015. Neonatal brain MRI segmentation: a review. Comput. Biol. Med. 64, 163–178.
Dice, L.R., 1945. Measures of the amount of ecologic association between species. Ecology 26 (3), 297–302.
Dittrich, E., Riklin-Raviv, T., Kasprian, G., Brugger, P., Prayer, D., Langs, G., 2011. Learning a spatio-temporal latent atlas for fetal brain segmentation. In: MICCAI Workshop on Image Analysis of Human Brain Development, pp. 9–16.
Eskildsen, S.F., Coupé, P., Fonov, V., Manjón, J.V., Leung, K.K., Guizard, N., Wassef, S.N., Stergaard, L.R., Collins, D.L., 2012. BEaST: brain extraction based on nonlocal segmentation technique. NeuroImage 59 (3), 2362–2373.
Fischl, B., Salat, D.H., Busa, E., Albert, M., Dieterich, M., Haselgrove, C., van der Kouwe, A., Killiany, R., Kennedy, D., Klaveness, S., Montillo, A., Makris, N., Rosen, B., Dale, A.M., 2002. Whole brain segmentation: automated labeling of neuroanatomical structures in the human brain. Neuron 33 (3), 341–355.
Gholipour, A., Akhondi-Asl, A., Estroff, J.A., Warfield, S.K., 2012. Multi-atlas multi-shape segmentation of fetal brain MRI for volumetric and morphometric analysis of ventriculomegaly. NeuroImage 60 (3), 1819–1831.
Gholipour, A., Estroff, J.A., Warfield, S.K., 2010. Robust super-resolution volume reconstruction from slice acquisitions: application to fetal brain MRI. IEEE Trans. Med. Imaging 29 (10), 1739–1758.
Gilmore, J.H., Lin, W., Prastawa, M.W., Looney, C.B., Vetsa, Y.S.K., Knickmeyer, R.C., Evans, D.D., Smith, J.K., Hamer, R.M., Lieberman, J.A., Gerig, G., 2007. Regional gray matter growth, sexual dimorphism, and cerebral asymmetry in the neonatal brain. J. Neurosci. 27 (6), 1255–1260.
Gousias, I.S., Edwards, A.D., Rutherford, M.A., Counsell, S.J., Hajnal, J.V., Rueckert, D., Hammers, A., 2012. Magnetic resonance imaging of the newborn brain: manual segmentation of labelled atlases in term-born and preterm infants. NeuroImage 62 (3), 1499–1509.
Gousias, I.S., Hammers, A., Counsell, S.J., Srinivasan, L., Rutherford, M.A., Heckemann, R.A., Hajnal, J.V., Rueckert, D., Edwards, A.D., 2013. Magnetic resonance imaging of the newborn brain: automatic segmentation of brain images into 50 anatomical regions. PLoS One 8 (4), e59990.
Gui, L., Lisowski, R., Faundez, T., Hüppi, P.S., Lazeyras, F., Kocher, M., 2012a. Morphology-based segmentation of newborn brain MR images. In: MICCAI Grand Challenge on Neonatal Brain Segmentation 2012 (NeoBrainS12), pp. 1–8.
Gui, L., Lisowski, R., Faundez, T., Hüppi, P.S., Lazeyras, F., Kocher, M., 2012b. Morphology-driven automatic segmentation of MR images of the neonatal brain. Med. Image Anal. 16 (8), 1565–1579.
Habas, P.A., Kim, K., Chandramohan, D., Rousseau, F., Glenn, O.A., Studholme, C., 2009. Statistical model of laminar structure for atlas-based segmentation of the fetal brain from in utero MR images. In: SPIE Medical Imaging. Image Processing, vol. 7259.
Habas, P.A., Kim, K., Corbett-Detig, J.M., Rousseau, F., Glenn, O.A., Barkovich, A.J., Studholme, C., 2010a. A spatiotemporal atlas of MR intensity, tissue probability and shape of the fetal brain with application to segmentation. NeuroImage 53 (2), 460–470.
Habas, P.A., Kim, K., Rousseau, F., Glenn, O.A., Barkovich, A.J., Studholme, C., 2008. Atlas-based segmentation of the germinal matrix from in utero clinical MRI of the fetal brain. Med. Image Comput. Comput. Assist. Interv. (MICCAI) 11 (1), 351–358.
Habas, P.A., Kim, K., Rousseau, F., Glenn, O.A., Barkovich, A.J., Studholme, C., 2010b. Atlas-based segmentation of developing tissues in the human brain with quantitative validation in young fetuses. Hum. Brain Mapp. 31 (9), 1348–1358.
Hack, M., Fanaroff, A.A., 2000. Outcomes of children of extremely low birthweight and gestational age in the 1990s. Seminars Neonatol. 5 (2), 89–106.
Haidar, H., Warfield, S.K., Soul, J.S., 2005. Talairach-based parcellation of neonatal brain magnetic resonance imaging data: validation of a new approach. J. Neuroimaging Off. J. Am. Soc. Neuroimaging 15 (4), 305–314.
Heckemann, R.A., Hajnal, J.V., Aljabar, P., Rueckert, D., Hammers, A., 2006. Automatic anatomical brain MRI segmentation combining label propagation and decision fusion. NeuroImage 33 (1), 115–126.
Hüppi, P.S., Schuknecht, B., Boesch, C., Bossi, E., Felblinger, J., Fusch, C., Herschkowitz, N., 1996. Structural and neurobehavioral delay in postnatal brain development of preterm infants. Pediatr. Res. 39 (5), 895–901.
Ison, M., Dittrich, E., Donner, R., Kasprian, G., Prayer, D., Langs, G., 2012. Fully automated brain extraction and orientation in raw fetal MRI. In: MICCAI Workshop on Paediatric and Perinatal Imaging 2012 (PaPI 2012).
Išgum, I., Benders, M.J.N.L., Avants, B., Cardoso, M.J., Counsell, S.J., Gomez, E.F., Gui, L., Hppi, P.S., Kersbergen, K.J., Makropoulos, A., Melbourne, A., Moeskops, P., Mol, C.P., Kuklisova-Murgasova, M., Rueckert, D., Schnabel, J.A., Srhoj-Egekher, V., Wu, J., Wang, S., de Vries, L.S., Viergever, M.A., 2015. Evaluation of automatic neonatal brain segmentation algorithms: the NeoBrainS12 challenge. Med. Image Anal. 20 (1), 135–151.
Jackson, D.C., Irwin, W., Dabbs, K., Lin, J.J., Jones, J.E., Hsu, D.A., Stafstrom, C.E., Seidenberg, M., Hermann, B.P., 2011. Ventricular enlargement in new-onset pediatric epilepsies. Epilepsia 52 (12), 2225–2232.
Jiang, S., Xue, H., Glover, A., Rutherford, M., Rueckert, D., Hajnal, J.V., 2007. MRI of moving subjects using multislice snapshot images with volume reconstruction (SVR): application to fetal, neonatal, and adult brain studies. IEEE Trans. Med. Imaging 26 (7), 967–980.
Jones, S.E., Buchbinder, B.R., Aharon, I., 2000. Three-dimensional mapping of cortical thickness using Laplace's equation. Hum. Brain Mapp. 11 (1), 12–32.
Justice, R., Stokely, E., 1996. 3-D segmentation of MR brain images using seeded region growing. In: IEEE Engineering in Medicine and Biology Society, vol. 3, pp. 1083–1084.

Kainz, B., Keraudren, K., Kyriakopoulou, V., Rutherford, M., Hajnal, J.V., Rueckert, D., 2014. Fast fully automatic brain detection in fetal MRI using dense rotation invariant image descriptors. In: IEEE International Symposium on Biomedical Imaging (ISBI), pp. 1230–1233.

Kamnitsas, K., Ledig, C., Newcombe, V.F.J., Simpson, J.P., Kane, A.D., Menon, D.K., Rueckert, D., Glocker, B., 2016. Efficient Multi-scale 3d CNN with Fully Connected CRF for Accurate Brain Lesion Segmentation arXiv:1603.05959.

Kass, M., Witkin, A., Terzopoulos, D., 1988. Snakes: active contour models. Int. J. Comput. Vis. 1 (4), 321–331.

Keraudren, K., Kuklisova-Murgasova, M., Kyriakopoulou, V., Malamateniou, C., Rutherford, M., Kainz, B., Hajnal, J., Rueckert, D., 2014. Automated fetal brain segmentation from 2d MRI slices for motion correction. NeuroImage 101, 633–643.

Kersbergen, K.J., Makropoulos, A., Aljabar, P., Groenendaal, F., de Vries, L.S., Counsell, S.J., Benders, M.J.N.L., 2016. Longitudinal regional brain development and clinical risk factors in extremely preterm infants. J. Pediatr. 178, 93–100 e6.

Keunen, K., Kersbergen, K.J., Groenendaal, F., Isgum, I., de Vries, L.S., Benders, M.J.N.L., 2012. Brain tissue volumes in preterm infants: prematurity, perinatal risk factors and neurodevelopmental outcome: a systematic review. J. Matern. Fetal neonatal Med. Off. J. Eur. Assoc. Perinat. Med. Fed. Asia Ocean. Perinat. Soc. Int. Soc. Perinat. Obstet. 25 (Suppl. 1), 89–100.

Kim, H., Lepage, C., Evans, A.C., Barkovich, A.J., Xu, D., 2015. NEOCIVET: Extraction of Cortical Surface and Analysis of Neonatal Gyrification Using a Modified CIVET Pipeline. Medical Image Computing and Computer-assisted Intervention (MICCAI), pp. 571–579.

Kim, K., Habas, P.A., Rousseau, F., Glenn, O.A., Barkovich, A.J., Studholme, C., 2010. Intersection based motion correction of multi-slice MRI for 3d in utero fetal brain image formation. Ieee Trans. Med. Imaging 29 (1), 146–158.

Kobashi, S., Udupa, J.K., 2013. Fuzzy connectedness image segmentation for newborn brain extraction in MR images. In: 2013 35th Annual International Conference of the IEEE Engineering in Medicine and Biology Society (EMBC), pp. 7136–7139.

Krizhevsky, A., Sutskever, I., Hinton, G.E., 2012. ImageNet classification with deep convolutional neural networks. In: Advances in Neural Information Processing Systems 25, pp. 1097–1105.

Kuklisova-Murgasova, M., Aljabar, P., Srinivasan, L., Counsell, S.J., Doria, V., Serag, A., Gousias, I.S., Boardman, J.P., Rutherford, M.A., Edwards, A.D., Hajnal, J.V., Rueckert, D., 2011. A dynamic 4d probabilistic atlas of the developing brain. NeuroImage 54 (4), 2750–2763.

Kuklisova-Murgasova, M., Quaghebeur, G., Rutherford, M.A., Hajnal, J.V., Schnabel, J.A., 2012. Reconstruction of fetal brain MRI with intensity matching and complete outlier removal. Med. Image Anal. 16 (8), 1550–1564.

Kyriakopoulou, V., Vatansever, D., Elkommos, S., Dawson, S., McGuinness, A., Allsop, J., Molnr, Z., Hajnal, J., Rutherford, M., 2014. Cortical overgrowth in fetuses with isolated ventriculomegaly. Cereb. Cortex (New York, N.Y. 1991) 24 (8), 2141–2150.

Ledig, C., Wright, R., Serag, A., Aljabar, P., Rueckert, D., 2012. Neonatal brain segmentation using second order neighborhood information. In: MICCAI Workshop on Perinatal and Paediatric Imaging (PaPI) 2012, pp. 33–40.

Liu, M., Kitsch, A., Miller, S., Chau, V., Poskitt, K., Rousseau, F., Shaw, D., Studholme, C., 2016. Patch-based augmentation of Expectation-Maximization for brain MRI tissue segmentation at arbitrary age after premature birth. NeuroImage 127, 387–408.

Lockwood Estrin, G., Kyriakopoulou, V., Makropoulos, A., Ball, G., Kuhendran, L., Chew, A., Hagberg, B., Martinez-Biarge, M., Allsop, J., Fox, M., Counsell, S.J., Rutherford, M.A., 2016. Altered white matter and cortical structure in neonates with antenatally diagnosed isolated ventriculomegaly. NeuroImage Clin. 11, 139–148.

Macqueen, J., 1967. Some methods of classification and analysis of multivariate observations. In: Proceedings of the Fifth Berkeley Symposium on Mathematical Statistics and Probability, pp. 281–297.

Mahapatra, D., 2012. Skull stripping of neonatal brain MRI: using prior shape information with graph cuts. J. Digital Imaging 25 (6), 802–814.

Makropoulos, A., Aljabar, P., Wright, R., Hüning, B., Merchant, N., Arichi, T., Tusor, N., Hajnal, J.V., Edwards, A.D., Counsell, S.J., Rueckert, D., 2016. Regional growth and atlasing of the developing human brain. NeuroImage 125, 456–478.

Makropoulos, A., Gousias, I., Ledig, C., Aljabar, P., Serag, A., Hajnal, J., Edwards, A., Counsell, S., Rueckert, D., 2014. Automatic whole brain MRI segmentation of the developing neonatal brain. IEEE Trans. Med. Imaging 33 (9), 1818–1831.

Makropoulos, A., Gousias, I., Ledig, C., Aljabar, P., Serag, A., Hajnal, J.V., Edwards, A.D., Counsell, S.J., Rueckert, D., 2012a. Automatic multi-label segmentation of the preterm brain with the use of adaptive atlases. In: International Society for Magnetic Resonance in Medicine (ISMRM).

Makropoulos, A., Ledig, C., Aljabar, P., Serag, A., Hajnal, J.V., Edwards, A.D., Counsell, S.J., Rueckert, D., 2012b. Automatic tissue and structural segmentation of neonatal brain MRI using expectation-maximization. In: MICCAI Grand Challenge on Neonatal Brain Segmentation 2012 (NeoBrainS12), pp. 9–15.

Malladi, R., Sethian, J., Vemuri, B., 1995. Shape modeling with front propagation: a level set approach. IEEE Trans. Pattern Anal. Mach. Intell. 17 (2), 158–175.

Mangin, J.-F., Frouin, V., Bloch, I., Régis, J., López-Krahe, J., 1995. From 3d magnetic resonance images to structural representations of the cortex topography using topology preserving deformations. J. Math. Imaging Vis. 5 (4), 297–318.

Marlow, N., Wolke, D., Bracewell, M.A., Samara, M., 2005. Neurologic and developmental disability at six years of age after extremely preterm birth. N. Engl. J. Med. 352 (1), 9–19.

Melbourne, A., Cardoso, M.J., Kendall, J.S., Robertson, N.J., Marlow, N., Ourselin, S., 2012. NeoBrainS12 Challenge: adaptive neonatal MRI brain segmentation with myelinated white matter class and automated extraction of ventricles I-IV. In: MICCAI Grand Challenge on Neonatal Brain Segmentation 2012 (NeoBrainS12), pp. 16–21.

Mewes, A.U.J., Hüppi, P.S., Als, H., Rybicki, F.J., Inder, T.E., McAnulty, G.B., Mulkern, R.V., Robertson, R.L., Rivkin, M.J., Warfield, S.K., 2006. Regional brain development in serial magnetic resonance imaging of low-risk preterm infants. Pediatrics 118 (1), 23–33.

Moeskops, P., Benders, M.J.N.L., Chiţ, S.M., Kersbergen, K.J., Groenendaal, F., de Vries, L.S., Viergever, M.A., Išgum, I., 2015. Automatic segmentation of MR brain images of preterm infants using supervised classification. NeuroImage 118, 628–641.

Moeskops, P., Viergever, M.A., Mendrik, A.M., de Vries, L.S., Benders, M.J.N.L., Isgum, I., 2016. Automatic segmentation of MR brain images with a convolutional neural network. IEEE Trans. Med. Imaging 35, 1252–1261.

Murphy, K., van der Aa, N.E., Negro, S., Groenendaal, F., de Vries, L.S., Viergever, M.A., Boylan, G.B., Benders, M.J.N.L., Išgum, I., 2017. Automatic quantification of ischemic injury on diffusion-weighted MRI of neonatal hypoxic ischemic encephalopathy. NeuroImage Clin. 14, 222–232.

Nie, D., Wang, L., Gao, Y., Sken, D., 2016. Fully convolutional networks for multi-modality isointense infant brain image segmentation. In: 2016 IEEE 13th International Symposium on Biomedical Imaging (ISBI), pp. 1342–1345.

Oishi, K., Mori, S., Donohue, P.K., Ernst, T., Anderson, L., Buchthal, S., Faria, A., Jiang, H., Li, X., Miller, M.I., van Zijl, P.C.M., Chang, L., 2011. Multi-contrast human neonatal brain atlas: application to normal neonate development analysis. NeuroImage 56 (1), 8–20.

Osher, S., Sethian, J.A., 1988. Fronts propagating with curvature-dependent speed: algorithms based on hamilton-jacobi formulations. J. Comput. Phys. 79 (1), 12–49.

Palmen, S.J.M.C., Hulshoff Pol, H.E., Kemner, C., Schnack, H.G., Durston, S., Lahuis, B.E., Kahn, R.S., Van Engeland, H., 2005. Increased gray-matter volume in medication-naive high-functioning children with autism spectrum disorder. Psychol. Med. 35 (4), 561–570.

Péporté, M., Ilea Ghita, D.E., Twomey, E., Whelan, P.F., 2011. A hybrid approach to brain extraction from premature infant MRI. In: Image Analysis, vol. 6688. Springer Berlin Heidelberg, Berlin, Heidelberg, pp. 719–730.

Peterson, B.S., Anderson, A.W., Ehrenkranz, R., Staib, L.H., Tageldin, M., Colson, E., Gore, J.C., Duncan, C.C., Makuch, R., Ment, L.R., 2003. Regional brain volumes and their later neurodevelopmental correlates in term and preterm infants. Pediatrics 111 (5), 939–948.

Pitas, I., 2000. Digital Image Processing Algorithms and Applications. Wiley-Blackwell, New York.

Prastawa, M., Gilmore, J.H., Lin, W., Gerig, G., 2005. Automatic segmentation of MR images of the developing newborn brain. Med. Image Anal. 9 (5), 457–466.

Pratt, W.K., 2007. Digital Image Processing: PIKS Scientific inside, 4 edition. Wiley-Interscience.

Rajchl, M., Lee, M.C.H., Oktay, O., Kamnitsas, K., Passerat-Palmbach, J., Bai, W., Damodaram, M., Rutherford, M.A., Hajnal, J.V., Kainz, B., Rueckert, D., 2016. DeepCut: Object Segmentation from Bounding Box Annotations Using Convolutional Neural Networks arXiv:1605.07866.

Rathbone, R., Counsell, S.J., Kapellou, O., Dyet, L., Kennea, N., Hajnal, J., Allsop, J.M., Cowan, F., Edwards, A.D., 2011. Perinatal cortical growth and childhood neurocognitive abilities. Neurology 77 (16), 1510–1517.

Rohlfing, T., Brandt, R., Menzel, R., Maurer Jr., C.R., 2004. Evaluation of atlas selection strategies for atlas-based image segmentation with application to confocal microscopy images of bee brains. NeuroImage 21 (4), 1428–1442.

Rousseau, F., Glenn, O.A., Iordanova, B., Rodriguez-Carranza, C., Vigneron, D.B., Barkovich, J.A., Studholme, C., 2006. Registration-based approach for reconstruction of high-resolution in utero fetal MR brain images. Acad. Radiol. 13 (9), 1072–1081.

Rousseau, F., Habas, P., Studholme, C., 2011. A supervised patch-based approach for human brain labeling. IEEE Trans. Med. Imaging 30 (10), 1852–1862.

Rutherford, M.A., 2002. MRI of the Neonatal Brain. W.B. Saunders.

Sanroma, G., Benkarim, O.M., Piella, G., Ballester, M. n. G., 2016. Building an ensemble of complementary segmentation methods by exploiting probabilistic estimates. In: Machine Learning in Medical Imaging, pp. 27–35.

Schuh, A., Murgasova, M., Makropoulos, A., Ledig, C., Counsell, S.J., Hajnal, J.V., Aljabar, P., Rueckert, D., 2015. Construction of a 4d brain atlas and growth model using diffeomorphic registration. In: MICCAI Workshop on Spatio-temporal Image Analysis for Longitudinal and Time-series Image Data, pp. 27–37.

Serag, A., Blesa, M., Moore, E.J., Pataky, R., Sparrow, S.A., Wilkinson, A.G., Macnaught, G., Semple, S.I., Boardman, J.P., 2016. Accurate Learning with Few Atlases (ALFA): an algorithm for MRI neonatal brain extraction and comparison with 11 publicly available methods. Sci. Rep. 6, 23470.

Serag, A., Kyriakopoulou, V., Rutherford, M.A., Edwards, A.D., Hajnal, J.V., Aljabar, P., Counsell, S.J., Boardman, J., Rueckert, D., 2012. A multi-channel 4d probabilistic atlas of the developing brain: application to fetuses and neonates. Ann. BMVA 2012 (3), 1–14.

Shattuck, D.W., Sandor-Leahy, S.R., Schaper, K.A., Rottenberg, D.A., Leahy, R.M., 2001. Magnetic resonance image tissue classification using a partial volume model. NeuroImage 13 (5), 856–876.

Shi, F., Fan, Y., Tang, S., Gilmore, J.H., Lin, W., Shen, D., 2010. Neonatal brain image segmentation in longitudinal MRI studies. NeuroImage 49 (1), 391–400.

Shi, F., Shen, D., Yap, P.-T., Fan, Y., Cheng, J.-Z., An, H., Wald, L.L., Gerig, G., Gilmore, J.H., Lin, W., 2011a. CENTS: cortical enhanced neonatal tissue segmentation. Hum. Brain Mapp. 32 (3), 382–396.

Shi, F., Wang, L., Dai, Y., Gilmore, J.H., Lin, W., Shen, D., 2012. LABEL: pediatric brain extraction using learning-based meta-algorithm. NeuroImage 62 (3), 1975–1986.

Shi, F., Wang, L., Wu, G., Li, G., Gilmore, J.H., Lin, W., Shen, D., 2014. Neonatal atlas construction using sparse representation. Hum. Brain Mapp. 35 (9), 4663–4677.

Shi, F., Yap, P.-T., Wu, G., Jia, H., Gilmore, J.H., Lin, W., Shen, D., 2011b. Infant brain atlases from neonates to 1- and 2-year-olds. PLoS One 6 (4), e18746.

Shiee, N., Bazin, P.-L., Cuzzocreo, J.L., Blitz, A., Pham, D.L., 2011. Segmentation of brain images using adaptive atlases with application to ventriculomegaly. In: Proceedings of the Information Processing in Medical Imaging, vol. 22, pp. 1–12.

Sijbers, J., Scheunders, P., Verhoye, M., van der Linden, A., van Dyck, D., Raman, E., 1997. Watershed-based segmentation of 3d MR data for volume quantization. Magn. Reson. Imaging 15 (6), 679–688.

Sled, J.G., Zijdenbos, A.P., Evans, A.C., 1998. A nonparametric method for automatic correction of intensity nonuniformity in MRI data. IEEE Trans. Med. Imaging 17 (1), 87–97.

Smith, S.M., 2002. Fast robust automated brain extraction. Hum. Brain Mapp. 17 (3), 143–155.

Song, Z., Tustison, N., Avants, B., Gee, J.C., 2006. Integrated graph cuts for brain MRI segmentation. Med. Image Comput. Comput. Assist. Interv. (MICCAI) 9 (2), 831–838.

Srhoj-Egekher, V., Benders, M.J., Kersbergen, K.J., Viergever, M.A., Isgum, I., 2012. Automatic segmentation of neonatal brain MRI using atlas based segmentation and machine learning approach. In: MICCAI Grand Challenge on Neonatal Brain Segmentation 2012 (NeoBrainS12), pp. 22–27.

Terzopoulos, D., Fleischer, K., 1988. Deformable models. Vis. Comput. 4 (6), 306–331.

Thompson, D.K., Warfield, S.K., Carlin, J.B., Pavlovic, M., Wang, H.X., Bear, M., Kean, M.J., Doyle, L.W., Egan, G.F., Inder, T.E., 2007. Perinatal risk factors altering regional brain structure in the preterm infant. Brain 130 (3), 667–677.

Thompson, D.K., Wood, S.J., Doyle, L.W., Warfield, S.K., Lodygensky, G.A., Anderson, P.J., Egan, G.F., Inder, T.E., 2008. Neonate hippocampal volumes: prematurity, perinatal predictors, and 2-year outcome. Ann. Neurol. 63 (5), 642–651.

Tofts, P., 2003. Quantitative MRI of the Brain: Measuring Changes Caused by Disease. Wiley.

Tourbier, S., Hagmann, P., Cagneaux, M., Guibaud, L., Gorthi, S., Schaer, M., Thiran, J.-P., Meuli, R., Bach Cuadra, M., 2015. Automatic brain extraction in fetal MRI using multi-atlas-based segmentation. In: SPIE Medical Imaging. Image Processing.

Tusor, N., Wusthoff, C., Smee, N., Merchant, N., Arichi, T., Allsop, J.M., Cowan, F.M., Azzopardi, D., Edwards, A.D., Counsell, S.J., 2012. Prediction of neurodevelopmental outcome after hypoxic-ischemic encephalopathy treated with hypothermia by diffusion tensor imaging analyzed using tract-based spatial statistics. Pediatr. Res. 72 (1), 63–69.

Tustison, N.J., Avants, B.B., Cook, P.A., Zheng, Y., Egan, A., Yushkevich, P.A., Gee, J.C., 2010. N4itk: improved N3 bias correction. IEEE Trans. Med. Imaging 29 (6), 1310–1320.

Tzourio-Mazoyer, N., Landeau, B., Papathanassiou, D., Crivello, F., Etard, O., Delcroix, N., Mazoyer, B., Joliot, M., 2002. Automated anatomical labeling of activations in SPM using a macroscopic anatomical parcellation of the MNI MRI single-subject brain. NeuroImage 15 (1), 273–289.

van der Knaap, M.S., Valk, J., Bakker, C.J., Schooneveld, M., Faber, J.A., Willemse, J., Gooskens, R.H., 1991. Myelination as an expression of the functional maturity of the brain. Dev. Med. Child Neurol. 33 (10), 849–857.

van der Lijn, F., den Heijer, T., Breteler, M.M.B., Niessen, W.J., 2008. Hippocampus segmentation in MR images using atlas registration, voxel classification, and graph cuts. NeuroImage 43 (4), 708–720.

Van Leemput, K., Maes, F., Vandermeulen, D., Suetens, P., 1999. Automated model-based tissue classification of MR images of the brain. IEEE Trans. Med. Imaging 18 (10), 897–908.

Wang, H., Das, S., Pluta, J., Craige, C., Altinay, M., Avants, B., Weiner, M., Mueller, S., Yushkevich, P., 2010. Standing on the shoulders of giants: improving medical image segmentation via bias correction. Med. Image Comput. Comput. Assist. Interv. (MICCAI) 13 (3), 105–112.

Wang, H., Suh, J.W., Das, S.R., Pluta, J., Craige, C., Yushkevich, P.A., 2012a. Multi-atlas segmentation with joint label fusion. IEEE Trans. Pattern Anal. Mach. Intell. 35 (3), 611–623.

Wang, L., Gao, Y., Shi, F., Li, G., Gilmore, J.H., Lin, W., Shen, D., 2015. LINKS: learning-based multi-source IntegratioN frameworK for Segmentation of infant brain images. NeuroImage 108, 160–172.

Wang, L., Shi, F., Li, G., Gao, Y., Lin, W., Gilmore, J.H., Shen, D., 2014. Segmentation of neonatal brain MR images using patch-driven level sets. NeuroImage 84C, 141–158.

Wang, L., Shi, F., Lin, W., Gilmore, J.H., Shen, D., 2011. Automatic segmentation of neonatal images using convex optimization and coupled level sets. NeuroImage 58 (3), 805–817.

Wang, L., Shi, F., Yap, P.-T., Gilmore, J.H., Lin, W., Shen, D., 2012b. 4d multi-modality tissue segmentation of serial infant images. PloS One 7 (9), e44596.

Wang, S., Kuklisova-Murgasova, M., Schnabel, J.A., 2012c. An atlas-based method for neonatal MR brain tissue segmentation. In: MICCAI Grand Challenge on Neonatal Brain Segmentation 2012 (NeoBrainS12), pp. 28–35.

Warfield, S.K., Zou, K.H., Wells, W.M., 2004. Simultaneous truth and performance level estimation (STAPLE): an algorithm for the validation of image segmentation. IEEE Trans. Med. Imaging 23 (7), 903–921.

Weisenfeld, N.I., Mewes, A.U.J., Warfield, S.K., 2006. Highly accurate segmentation of brain tissue and subcortical gray matter from newborn MRI. Med. Image Comput. Comput. Assist. Interv. (MICCAI) 9 (1), 199–206.

Weisenfeld, N.I., Warfield, S.K., 2009. Automatic segmentation of newborn brain MRI. NeuroImage 47 (2), 564–572.

Weishaupt, D., Froehlich, J.M., Nanz, D., Köchli, V.D., Pruessmann, K.P., Marincek, B., 2008. How Does MRI Work?: an Introduction to the Physics and Function of Magnetic Resonance Imaging. Springer.

Weisstanner, C., Kasprian, G., Gruber, G.M., Brugger, P.C., Prayer, D., 2015. MRI of the fetal brain. Clin. Neuroradiol. 25 (Suppl. 2), 189–196.

Wells, W.M., Grimson, W.L., Kikinis, R., Jolesz, F.A., 1996. Adaptive segmentation of MRI data. IEEE Trans. Med. Imaging 15 (4), 429–442.

Wolz, R., Aljabar, P., Hajnal, J.V., Hammers, A., Rueckert, D., 2010. LEAP: learning embeddings for atlas propagation. NeuroImage 49 (2), 1316–1325.

Wright, I.C., Rabe-Hesketh, S., Woodruff, P.W., David, A.S., Murray, R.M., Bullmore, E.T., 2000. Meta-analysis of regional brain volumes in schizophrenia. Am. J. Psychiatry 157 (1), 16–25.

Wright, R., Kyriakopoulou, V., Ledig, C., Rutherford, M., Hajnal, J., Rueckert, D., Aljabar, P., 2014. Automatic quantification of normal cortical folding patterns from fetal brain MRI. NeuroImage 91, 21–32.

Wu, J., Ashtari, M., Betancourt, L.M., Brodsky, N.L., Giannetta, J.M., Gee, J.C., Hurt, H., Avants, B.B., 2014. Cortical Parcellation for Neonatal Brains. IEEE, pp. 1377–1380.

Wu, J., Avants, B., 2012. Automatic registration-based segmentation for neonatal brains using ANTs and Atropos. In: MICCAI Grand Challenge on Neonatal Brain Segmentation 2012 (NeoBrainS12), pp. 36–47.

Xue, H., Srinivasan, L., Jiang, S., Rutherford, M., Edwards, A.D., Rueckert, D., Hajnal, J.V., 2007. Automatic segmentation and reconstruction of the cortex from neonatal MRI. NeuroImage 38 (3), 461–477.

Yamaguchi, K., Fujimoto, Y., Kobashi, S., Wakata, Y., Ishikura, R., Kuramoto, K., Imawaki, S., Hirota, S., Hata, Y., 2010. Automated fuzzy logic based skull stripping in neonatal and infantile MR images. In: IEEE International Conference on Fuzzy Systems (FUZZ). IEEE, pp. 1–7.

Yu-qian, Z., Wei-hua, G., Zhen-cheng, C., Jing-tian, T., Ling-yun, L., 2005. Medical images edge detection based on mathematical morphology. In: IEEE Engineering in Medicine and Biology Society, pp. 6492–6495.

Zaitsev, M., Maclaren, J., Herbst, M., 2015. Motion artefacts in MRI: a complex problem with many partial solutions. Journal of magnetic resonance imaging. JMRI 42 (4), 887–901.

Zeng, X., Staib, L.H., Schultz, R.T., Duncan, J.S., 1999. Segmentation and measurement of the cortex from 3-D MR images using coupled-surfaces propagation. IEEE Trans. Med. Imaging 18 (10), 927–937.

Zhang, W., Li, R., Deng, H., Wang, L., Lin, W., Ji, S., Shen, D., 2015. Deep convolutional neural networks for multi-modality isointense infant brain image segmentation. NeuroImage 108, 214–224.

Zhang, Y., Shi, F., Yap, P.-T., Shen, D., 2016. Detail-preserving construction of neonatal brain atlases in space-frequency domain: detail-Preserving Construction of Neonatal Brain Atlases. Hum. Brain Mapp. 37 (6), 2133–2150.